Universidade de Aveiro Departamento de Eletrónica, Telecomunicações e Informática
2019

TIAGO JOÃO ALMEIDA GOMES

LIDAR para regiões de interesse

REGION OF INTEREST LIDAR

Universidade de Aveiro
2019

Departamento de Eletrónica,
Telecomunicações e Informática

TIAGO JOÃO ALMEIDA GOMES

LIDAR para regiões de interesse

REGION OF INTEREST LIDAR

Dissertação apresentada à Universidade de Aveiro para cumprimento dos requisitos necessários à obtenção do grau de Mestre em Engenharia Eletrónica e Telecomunicações, realizada sob a orientação científica do Doutor Paulo Monteiro, Professor Associado do Departamento de Eletrónica, Telecomunicações e Informática da Universidade de Aveiro, e do Doutor Miguel Drummond, Investigador Auxiliar do Instituto de Telecomunicações.

Dedico este trabalho aos meus pais e a minha irmã.

o júri / the jury

presidente / president — Professor Doutor João Nuno Pimentel da Silva Matos
professor associado da Universidade de Aveiro

vogais / examiners committee — Prof. Doutora Maria do Carmo Raposo de Medeiros
professora associada da Faculdade de Ciências e Tecnologia da Universidade de Coimbra

Prof. Doutor Paulo Miguel Nepomuceno Pereira Monteiro
professor associado da Universidade de Aveiro

agradecimentos / acknowledgements

Aproveito esta oportunidade para poder agradecer ao meus pais, à minha irmã, a todos os outros familiares e amigos que me apoiaram no decorrer desta dissertação de mestrado. Aproveito também para agradecer ao professor Paulo Monteiro, Miguel Drummond e a Abel Lorences pela disponibilidade e paciência.

Agradeço também ao Instituto de Telecomunicações, a Bosch Car Multimedia Portugal, assim como ao projetos Landmark (POCI-01-0145-FEDER-031527); RETIOT (POCI-01-0145-FEDER-016432) e SOFTLI (Software defined LIDAR).

Palavras Chave LiDAR, automóvel, região de interesse, óptica geométrica, campo de visão

Resumo

Neste documento é apresentado o trabalho desenvolvido na tese de mestrado sobre "LIDAR para regiões de interesse". O objetivo é desenvolver um LiDAR capaz de caracterizar uma região de interesse com elevada precisão. Tendo em conta o erro elevado num LiDAR por triangulação, para grandes distâncias, um LiDAR para regiões de interesse conseguiria complementar um LiDAR por triangulação fazendo, com que seja possível distinguir diferentes pontos a grandes distâncias.

Este LiDAR é validado usando uma ferramenta de simulação desenvolvida em Matlab ao longo da dissertação, baseada num sistema constituido por um espelho, uma lente e um sensor, onde todos os parâmetros definidos, desde o diametro da lente, a distância focal da lente, a distância entre espelho e lente e tamanho do sensor influenciam os resultados, estes valores foram definidos através de diferentes testes de modo a que com os valores definidos fosse possível atingir os objetivos desta tese.

Este trabalho mostra, teoricamente, que um ROI LiDAR é fazível e viável, sendo uma opção a considerar para a indústria automóvel, completando assim um LiDAR por triangulação.

Keywords LiDAR, automotive, region of interest, ray optics, field of view

Abstract

In this document is presented the work developed in the master thesis on "Region of Interest LiDAR". The goal is to develop a LiDAR capable of characterizing a region of interest with high precision. Taking into account the high error in a triangulation LiDAR for great distances, an ROI LiDAR could be able to complement a triangulation LiDAR, making it possible to distinguish different spots at great distances.

This LiDAR is validated using a simulation tool developed in Matlab throughout the thesis, based on a system consisting of a mirror, a lens and a sensor, where all defined parameters, from lens diameter, the focal length of the lens, the distance between mirror and lens and sensor size influence the results. These values were defined through different tests so that, with the defined values, it was possible to achieve the objectives of this thesis.

This work theoretically shows that a LiDAR ROI is doable and feasible, being an option to consider for the automotive industry, completing a triangular LiDAR.

Contents

List of Figures

List of Tables

Glossary

ADAS	Advanced Driver Assistance System
CEO	Chief Executive Officer
FoV	Field of View
GPS	Global Positioning System
LIDAR	Light Detection And Ranging
MEMs	Microelectromechanical systems
NHTSA	National Highway Traffic Safety Administration
ROI	Region of Interest
RADAR	Radio Detection and Ranging
ToF	Time of Flight

CHAPTER 1

Introduction

Since the beginning of humanity as a society, Man has always been looking for evolution, inventing new things to improve lifestyle and increase comfort, being one of these great inventions the wheel. Since the invention of the wheel, the evolution around it has been so great that Man has reached motorized cars. And the question that is always being asked is, what's next? Considering the number of accidents, and consequent deaths or injuries, that according to the association for safe international travel per year there are nearly 1.25 million deaths, an average of 3287 per day, and 20 to 50 million people injured or disabled [1]. So considering the human tendency to evolve and the need to reduce the number of casualties in car related accidents, most being due to human error, a fully self-driving car is a very good solution. Such car needs a system that allows the car to drive itself using the help of different sensors.

One technology, among others, that has a particular interest, is LiDAR technology. LiDAR stands for Light Detection And Ranging, and as we will see in the chapter dedicated to the State of the Art, LiDAR has an important role in the development of self-driving cars, since this technology allows a self-driving car to analyze better what's happening around it and to act accordingly, what will help decrease the number of accidents. LiDAR gives the car the ability to see at great distances, but sometimes at great distances it may be difficult to distinguish some points, and that's when ROI LiDAR (Region of Interest) becomes important in a self-driving vehicle, since by defining an ROI it will help the car to better see to that point and distinguish points that otherwise wouldn't be distinguished, this happens because an ROI can be defined in image processing as the boundaries of an object under consideration [2], and so by defining an ROI it will help a self-driving car to better steer itself depending on the scenario.

1.1 Triangulation LiDAR and associated problem

Triangulation LiDAR is a geometrical approach for the estimation of a spot's distance considering a certain referential [3]. For that purpose are considered two "observers" at a known distance from each other, and a third point that represents the spot whose distance has to be estimated. This theme is studied in a thesis which the title is "Spatial Domain LiDAR" [4]. The test setup used in this thesis consists of two cameras distanced of 1.2m, a Field of View (FoV) of 45° and camera sensors with 2000 pixels length. FoV is the angular extent of a certain scene that can be imaged by a camera [5]. In this case, FoV divided by the pixel length gives 0.0225° per pixel. A layout of a Triangulation LiDAR is presented in Figure 1.1, where it is also represented the Dark Zone of the system, this zone is outside the FoV of both cameras.

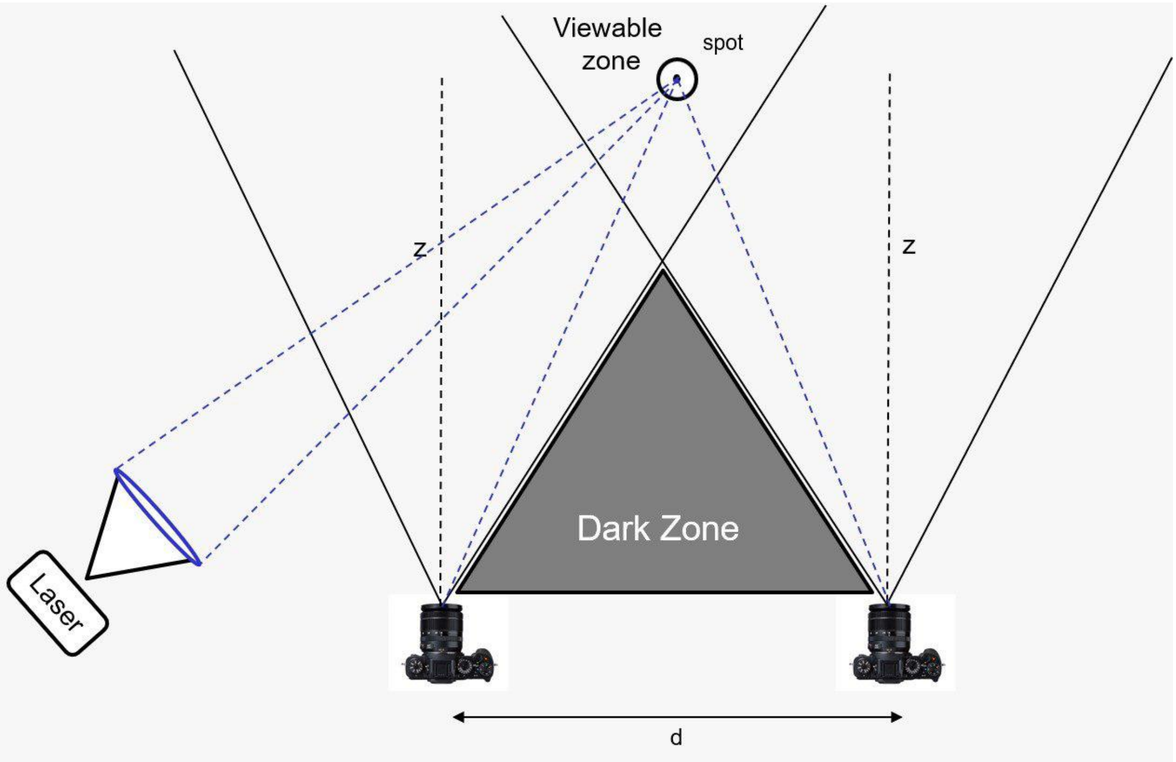

Figure 1.1: Triangulation LiDAR example [4].

In the tests made, it was found that the greater the distance the greater the error on the estimation would be, this error is due to a super-linear variation with the distance[4]. The main reason for this problem was the low sensor resolution, so the solution would be to increase resolution above the resolution of the sensor. Solutions for addressing such problem are referred to as geometrical super-resolution [6].

This super-resolution method consists on creating bigger spots, this is achieved by considering pairs of spots instead of one single spot. The tests made for this case showed that the error still increases with the distance between the two cameras and the target in spite of a bigger spot. In Figure 1.2 is possible to observe the behavior of the error with the increase of the distance.

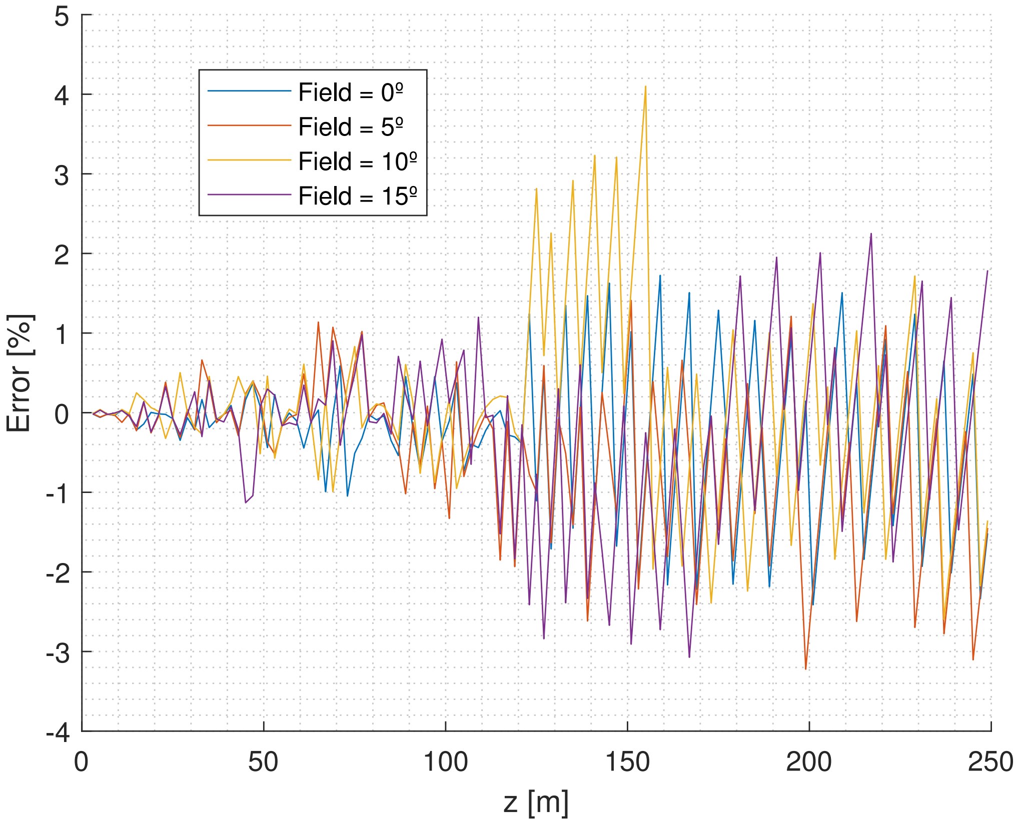

Figure 1.2: Error vs Distance for different fields [4].

1.1.1 Solution

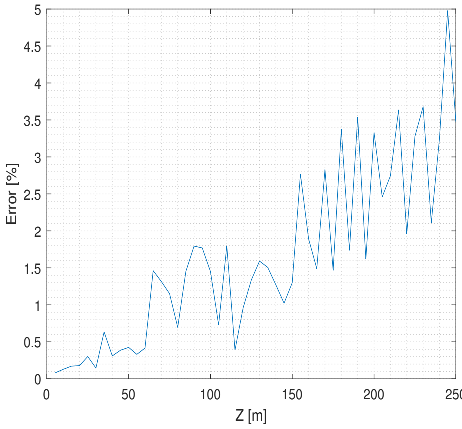

(a) Maximum error for all fields, considering a FoV per pixel of 0.025° .

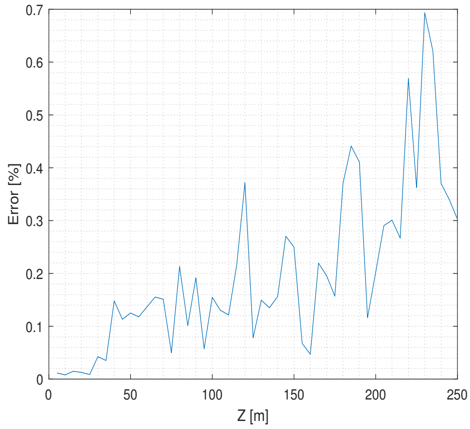

(b) Maximum error for all fields, considering a FoV per pixel of 0.0025°

Figure 1.3: Maximum error for all fields, considering a FoV per pixel of 0.025° and 0.0025°

Figure 1.3a and 1.3b, show the maximum error for all fields, considering a FoV per pixel of 0.025° and 0.0025° respectively. In 1.3a it's possible to observe that the error increases significantly for distances exceeding approximately 150m, reaching a 5% error near 250m, but if this FoV is ten times better (Figure 1.3b) the maximum value for the error is only 0.7%. Therefore, with this in mind, a solution emerged, develop a LiDAR that is able do characterize a ROI, with a target FoV per pixel of 0.0025°. This LiDAR could be used for complementing a cheap LiDAR with a broad FoV per pixel.

1.2 Motivation

In order to meet this objective, was developed using Matlab, a simulation tool that was able to characterize an ROI, based on a tuneable 2D mirror, that works like an human eye, it "looks" to the ROI, making it easier to define a ROI. Tests were made in order to find the best possible scheme to define a ROI in order to prove that the simulation tool was working as expected and baring in mind that a ROI LiDAR would be used in a car, so the scheme had to fit in a car. After these tests, another tests were made in order to find the parameters values to meet the objectives, and to see if with those values was possible to do a real setup, like it was already considered in the first tests. This simulation tool considered a spot or more than one spot distanced from the mirror, and the mirror would feed a sensor with the reflection of the spots considered.

The initial idea was to make a simulator using Matlab in order to simulate a system of a mirror and sensor, in order to characterize an ROI. Later a lens was also added, so it is necessary to define a focal length. Initially, the concepts necessary to make a simulation of a mirror, a lens and a sensor in Matlab, were studied. In short a system that received several sources points, with a configurable distance between mirror and lens and a configurable focal length. The distance between point sources and the mirror can also be configurable.

1.3 Objectives

The main target of this thesis is to develop a ROI LiDAR capable of characterizing a region of interest, to tell a precise distance to the obstacle.

All objectives that were pursued are as follows:

1. Develop a ray tracing simulator capable of representing a image that a spot (or several spots) produce in a sensor, being fed by a mirror and an ideal lens.
2. Numerically validate that using ROI LiDAR works.
3. Using the simulator to obtain a FoV of 0.0025º.
4. Find a LiDAR equation to prove that the system in question can work in real environments.

1.4 Contributions

The main contributions of the work developed in this thesis are the following

1. A ray optics simulator tool;
2. Numerical demonstration that a ROI LiDAR is doable;
3. Solution to the problem found in Triangulation LiDAR associated to great distances.

CHAPTER 2

State of The Art

It was made a classification system by NHTSA, a classification system, in which the 6 different levels of autonomy were defined, ranging from Level 0, no automation, to Level 5, full automation, as it is possible to observe on Figure 2.1

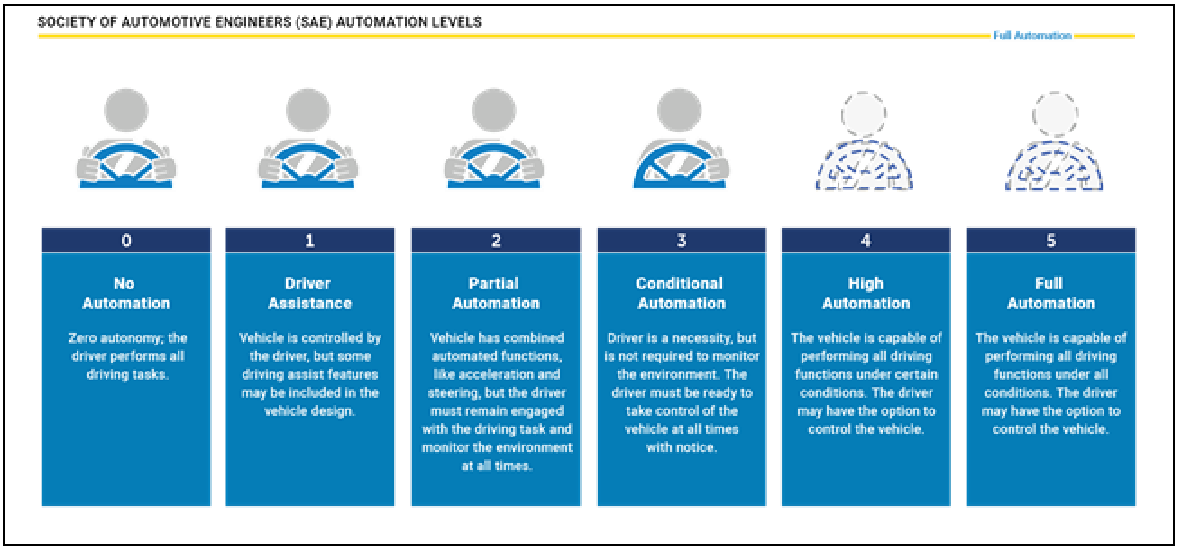

Figure 2.1: Automation Levels [7].

To be able to reach a fully autonomous vehicle, its system needs something that can act like the human eyes, so that with the information the car sees, the system can make decisions about what to do, taking into account what kind of object the car is "seeing", it's trajectory and the distance to the object. Until now there are mainly three options to be the car eyes, RADAR, LiDAR and cameras. These three options can be used ate the same time, or a combination of some of them, which can make a difference in the Level of autonomy of the vehicle.

2.1 Main sensors in autonomous vehicles

The objective is to achieve a self-driving car, in order to do so the cars need to use different sensors to use them as "eyes" to see around the car and using computer vision algorithms, act accordingly. This section describes some of the sensors used in autonomous cars.

2.1.1 LiDAR

LiDAR is a light detection technology that uses a pulsed laser light to collect measurements. Usually it works with ToF, it calculates how long a signal takes to return to the sensor after being sent and reflected by an object [8]. The distance between the LiDAR and the object is then calculated dividing the speed of light with half of the time that the signal took from emission and reception.

Using LiDAR it is possible to make a 3D map all around the sensor, and it is called a 'Point Cloud'. A Point Cloud is a cluster of points, each with its 3D coordinates [9], which gives a 3D representation of the surroundings. Using a Point Cloud alone, it is often possible with just a LiDAR distinguish various different objects from each other, and because of the short light pulses, LiDAR is able to detect small objects.

One of the disadvantages of the LiDAR technology is that the use at night or in bad weather is conditioned. The other disadvantage is the price, since a single Lidar may reach the values of thousands of euros. More recently, some LiDAR companies like Luminar's, has announced an lower-price alternative to current LiDAR systems. This LiDAR is called Iris LiDAR, and is said to cost less that 1000 dollars, (roughly 904 euros), for production vehicles or 500 dollars, (roughly 452 euros), for limited versions [10].

2.1.2 RADAR

RADAR is a detection system that uses radio waves to determine the range, angle, or velocity of objects. [11]. Normally it operates in the microwave region or in the ultra-high-frequency [12].

RADAR consists of a transmitter, a transmitting and receiving antenna, a receiver and a processor in order to determine properties of the object [11].

One way to determinate distance using RADAR is using ToF principle like in LiDAR, the only difference is the type of signal sent.

The price of a RADAR is much lower than the price of the LiDAR. But in terms of accuracy, LiDAR is better than RADAR, mainly due to the Point Cloud that a LiDAR can generate, making it possible to obtain more accurate results when implemented into AI (artificial intelligence) and machine learning algorithms. LiDAR can also detect smaller objects than RADAR, because of the short light pulses, already mentioned on the LiDAR subsection.

RADAR is better than LiDAR in the nighttime and in lousy weather conditions, like rain and fog, due to the radio waves are more resilient than light , making it not sensitive to different weather conditions and lack of light. The operating distance of the RADAR is also bigger than the operating distance of the LiDAR [13]

2.1.3 Camera

Cameras are often referred as "The Eyes of Autonomous Vehicles". Using cameras, cars can see a clear picture of the surroundings, like humans do looking through a camera [14].

Cameras are able to differentiate the colors of traffic lights, lane markings, different road signs, which is a big advantage from others technologies in self-driving cars because, the ability to read signs and see colors will allow cars to navigate modern roads without driver input. Another big advantage is the price, for example, comparing with the price of a LiDAR, it is possible to see that cameras are cheaper than a LiDAR, even if the processing power needed to analyze all the data from the cameras is expensive. The two combined (cameras and processor) are still cheaper than a LiDAR [14].

2.1.4 Ultrasonic sensors

Ultrasonic sensors operate by transmitting short bursts of sound waves, and using ToF to measure the distance to the object. This kind of sensors are usually used for parking assistance, self-parking, blind-spot detection, and in more recent vehicles it is used to open the trunk hands-free [15]. Ultrasonic sensors have a short-range, usually, less than 5m.

2.1.5 Interplay between sensors

Nowadays there are already many companies that have self-driving capabilities implemented in their cars, like Tesla for example, or other companies that have systems that applied to cars make them able to be autonomous, like Waymo for example.

Even though some companies don't use all the sensors mentioned in the previous subsections at the same time , analyzing the advantages and disadvantages of each sensor, it can be said that when counting with all types of sensors in the car, the Level 5 of autonomy will be closer to happening. For example, a self-driving car can use a LiDAR to generate detailed maps of the surroundings of the car. Even doing it in 3D, detecting a different kind of objects, making it safer to steer the car in a driving environment, and can also help make decisions, since, for example, Waymo system can detect the movement of the others cars, bicycles or pedestrians. It can use RADAR to determinate the speed to the other objects and distance to them, ultrasonic sensors to help the car park and camera to differentiate lane markings, road signs, traffic lights, acting as the eyes of the car.

2.2 Self-driving vehicles

As it was referred, there are a lot of companies that already have self-driving car capabilities implemented in their cars, like Tesla or Audi. Or in other case, some companies develop systems that can make a normal car become a self-driving car when applied to cars produced by car making companies, like Waymo or Uber.

2.2.1 Tesla

When Tesla launched the Tesla model S in 2014, it came with a new feature, Autopilot was included in the "Tech Package" option [16].

The Tesla Autopilot is a Level 2 semi-autonomous driving, and at this level it still requires a driver, since the vehicle in not capable of full autonomous driving [17]. Drivers can leave the hands off the steering wheel for some time, even though now the current version of Autopilot requires the driver to touch the steering wheel more often than previous versions [16]. But, even if the driver does not touch the steering wheel the car is able to steer, accelerate and brake automatically within its lane [18].

Tesla cars use 12 long-range ultrasonic sensors placed around the car, a forward radar that provides extra data about the surroundings of the car, that works in a redundant wavelength that makes it possible to see in strong rains, fog and dust, and 8 cameras around the car. As it is described in Tesla's website [18], the narrow frontal camera has a maximum range of 250 m, the main frontal camera, 150m, wide front camera, 60 m, the lateral cameras facing forwards, 80 m, the rear-facing camera as a maximum range of 50m, and the lateral cameras facing the backwards have a maximum range of 100 m. The radar used as maximum range of 160 m and the ultrasonic sensors have a maximum range of 8 m, as it is possible to see in Fig.2.2.

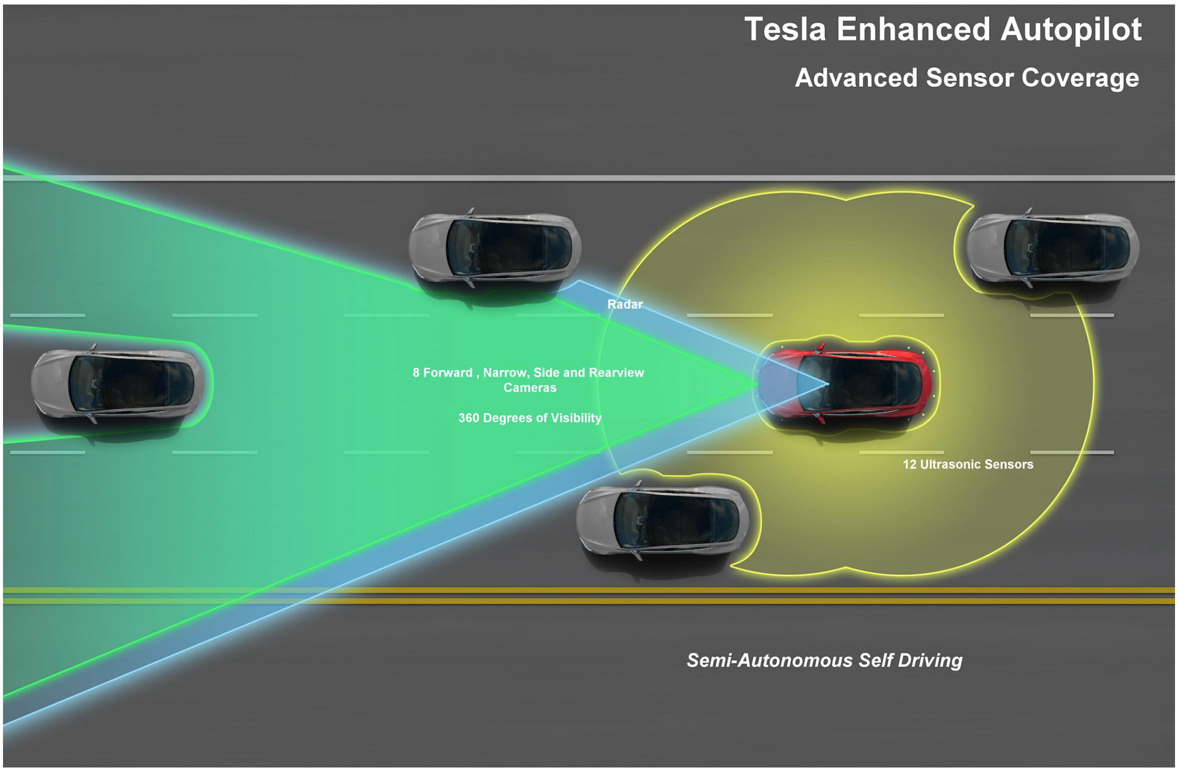

Figure 2.2: Illustration of Tesla's enhanced Autopilot [17].

Elon Musk, CEO of Tesla motors, says that LIDAR is not necessary to make Tesla automobiles fully capable of self-driving. "Tesla expects to have full self-driving cars" by 2020 [19].

2.2.2 Audi

In 2017 Audi announced a car with Level 3 of autonomy, the first to meet this Level, the Audi A8, the Audi AI traffic jam pilot. It is not a self-driving car that can be used in all kind of situations, but it is a system that can take charge in simple situations, being able to be in full control at speeds up to 60 km/h, on "highways or multi-lane road with barrier between oncoming lanes". The system, traffic jam pilot, is capable handling the full driving task, and when certain conditions are met, the driver can take his hands off the steering wheel, unlike on Level 2 cars [20]. The system is activated with an AI button on the center console, once the car is in the traffic jam pilot, the button lights up in green, and the virtual cockpit shows a stylized view of the car, like in Figure 2.3.

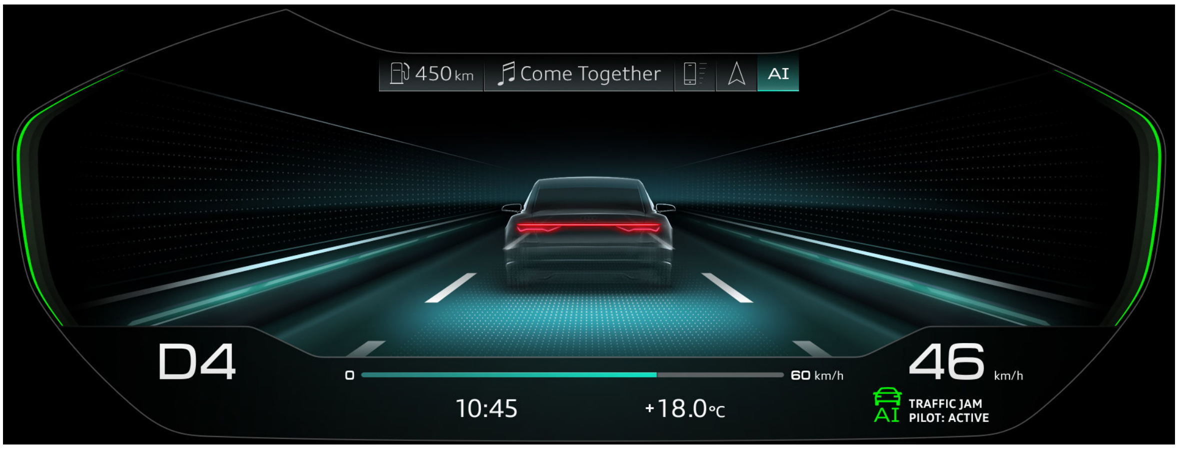

Figure 2.3: Audi virtual cockpit stylized [20].

The traffic jam pilot requires a highly detailed collection of data about the surroundings of the car, and for that it combines the use of ultrasonic sensors, cameras, radar and laser scanner [20].

2.2.3 Waymo

Waymo is a self-driving technology company, instead of making a full car, they just used their self-driving technology in other cars to make them capable of self-driving. Waymo uses LiDAR in order to build a picture of the surroundings of the car, RADAR for determinate the distance and speed of other objects, and it uses a camera to detect visual information [21]

According to John Krafic (Waymo CEO), their sensors provide vehicles with 360° FoV. The LiDAR that it is used in their equipment is able to map objects around the car in 3D and detect objects up to 300 meters away, and it can also 'see' underneath and around vehicles due to the short light pulses that LiDAR sends, picking up objects that a human driver could miss [22]. LiDAR sensors allow self-driving cars to classify and detect various objects, like cars, signs, lane markings, pedestrians and bicycles [23], as it is possible to observe in Figure 2.4.

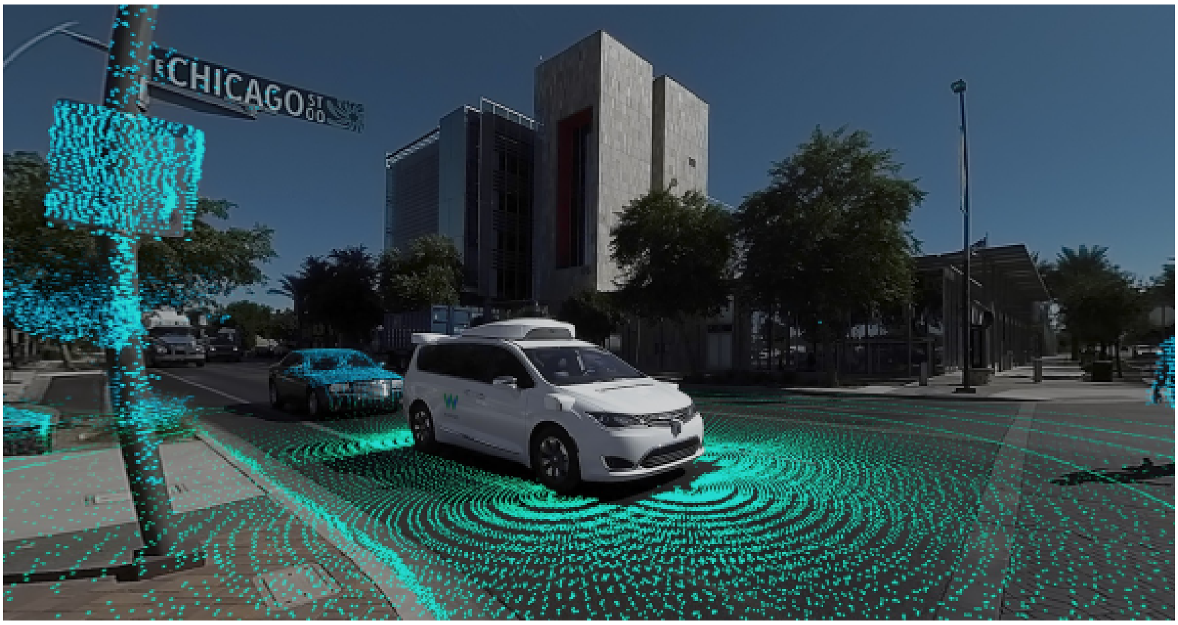

Figure 2.4: Illustration of Waymo LiDAR [24].

Using all the data gathered by the sensor, Waymo software can predict the movement of everything around the car, based on speed and trajectory.

Waymo technology is now being used by Chrysler Pacifica Hybrid, and since March 2018, the Jaguar I-Pace SUVs [22].

2.2.4 Uber

Uber, a well-known transportation company, that in 2016 launched its first self-driving car for their Uber Ride service, using Ford cars [25]. These cars used 20 cameras all around the vehicle, a GPS, radar and LiDAR [26], making the car able to construct a 3D image about its surroundings. The car used by Uber and the equipment necessary to the self-driving is in Figure 2.5.

Figure 2.5: Uber Self-Driving car [26].

2.3 2D Mirrors (MEMs Mirrors)

MEMS mirrors can steer, modulate, and switch light, as well as control the wavefront for focusing or phase modulation [27] This type of mirrors are tiny solid-state mirrors (mirror on a chip) that can work in one or two dimensions. For example, considering a laser, if the laser beam is pointed at the mirror it is precisely deflected and steered by the mirror to reach a target [28]. This kind of mirrors are important for this dissertation, because in order to maintain the total FoV the same as the one in triangulation LiDAR, and decrease the FoV per pixel it's needed a tunable element, and this element is the mirror.

Some companies that sell this type of MEMs mirrors are for example, Mirrorcle, Hamamatsu, ZhiSensor and Optotune. These companies were analyzed to choose which one would be the more appropriate for our application. MEMs mirror from Mirrorcle Technologies, have a diameter of 1 mm to 7.5 mm [29]. Mirrors from Hamamatsu in 2D only has a diameter of 1.23 mm [30]. Maradin has e different 2D MEMs mirrors, the MAR1100 has a diameter of 1 mm [31], and the Mar1800 has a size of 3.6x8.5 mm[32] . ZhiSensor has 4 different types of MEMs Mirrors, the name of these models are C1130, C1100, C2110 and C2120, with a diameter that varies from 3 mm, 1.3 mm and 1 mm, depending on the chosen models [33].The diameter of the Mirrors from the companies mentioned above are too small which can difficult the objective of the thesis, since the smaller the diameter the less light the mirror will get, that has impact on the FoV and as a consequence the system will get less light. But, the mirror from Optotune, the MI-15-30, has a diameter of 15 mm which is bigger than the ones mentioned before, which means that the system will get more light and a better FoV, with that in mind, the mirror from Optotune is the mirror more adequate for our application.

2.3.1 Optotune Mirror

In order to obtain such a LiDAR, it was chosen a mirror that will feed a sensor. The mirror chosen was the Optotune Mirror MR-15-30, a dual-axis mirror with position feedback.

The diameter of the mirror is 15mm ,and it can achieve a +/- 25° mechanical tilt, which results in an optical deflection of +/- 50°. The position feedback system of the mirror is accurately controlled with a standard PID controller[34].

As it is referred in the datasheet of the mirror, it is compact, which makes it suitable for practical applications, precise and has a large scan angle, and these are some advantages of the mirror. It can be used for Automotive applications, for example, LiDAR applications, dynamic headlights and ADAS[34].

As shown in the next table, taken from the mirror datasheet, the diameter of the mirror is 15 mm, with an external diameter of 35.4 mm and a total height of 14.5 mm. The resolution, in a closed-loop, is of $5\mu rad$, (approximately 0.0002865°) and a repeatability of 30 to $100\mu rad$.

Mechanical specifications

Actuator Type	4-Quandrant (2 axis, bi-directional)	
Mechanical tilt angle DC	±25 X axis; ±25 Y axis	°
Mechanical tilt angle dynamic	±25 X axis; ±25 Y axis	°
Mirror diameter	15	mm
Center of rotation to mirror surface	1.3	mm
External diameter	35.4	mm
Height	14.5	mm
Weight	29.3	g
Scale drift	T.B.D	ppm/°C (Max)
Zero drift	25	µrad/°C (Max)
Resolution (closed loop)	<5	µrad
Repeatability RMS (typical)	30-100	µrad
Full scale bandwidth Sine wave (±25°)	20	Hz
Small signal bandwidth (< ±0.1°)	350	Hz
Large angle step response (20° step)	7.5	ms
Small angle step response (0.1° step)	1.4	ms
Mechanical clamping	screws	
Magnetic shielding	yes	

Table 2.1: Mechanical specifications of the mirror [34].

CHAPTER 3

System Architecture

In order to represent the behavior of a mirror in Matlab, the Laws of Reflection were revisited. Considering an incident ray in a boundary surface, not all of the incident light is transmitted, a portion of the light is reflected, not changing medium. [35]. Taking into account Snell's Law,

$$\frac{\sin\theta_{out}}{\sin\theta_{in}} = \frac{n_1}{n_2}. \tag{3.1}$$

Since the medium is the same,

$$\frac{\sin\theta_{out}}{\sin\theta_{in}} = 1. \tag{3.2}$$

Then the relationship between incident and reflected angle is as follows,

$$\theta_{in} = -\theta_{out}. \tag{3.3}$$

In our case we are using a Mirror as illustrated in Figure 3.1.

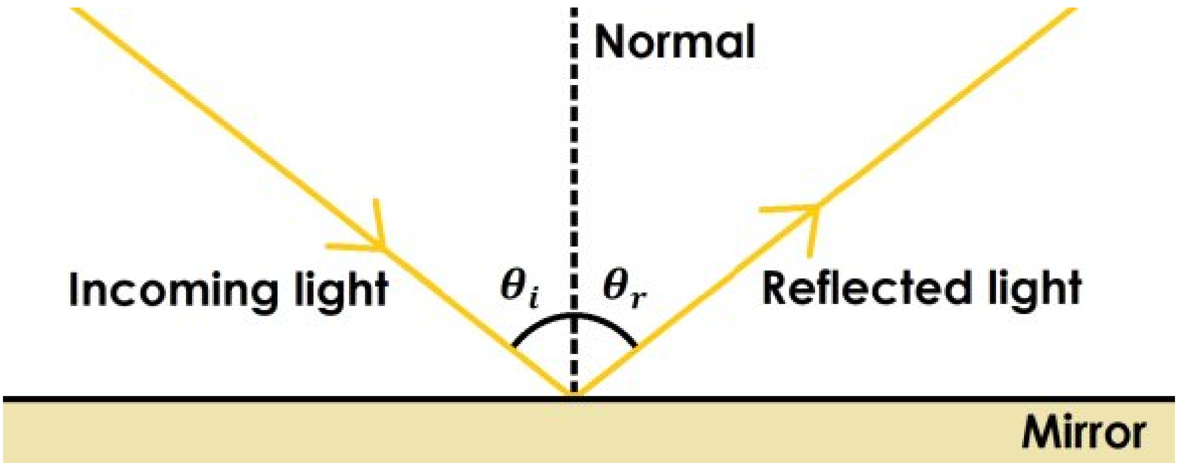

Figure 3.1: Reflection Laws Diagram [36].

Since the chosen mirror has a rotating motion, it is also necessary to consider the case were the mirror has a tilt. A mirror that makes a rotation through a given angle, the beam of reflected light from it will rotate through an angle of 2 times the angle of rotation [37], and this is represented in Figure 3.2.

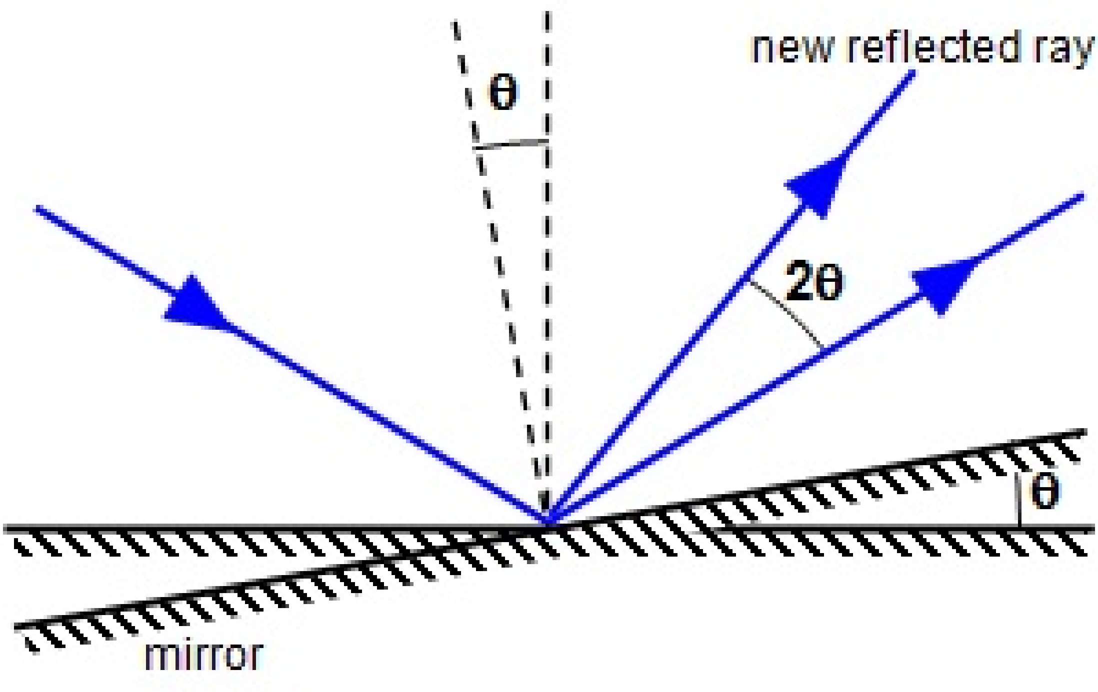

Figure 3.2: Reflection Laws Diagram with tilt [37].

The simulations were all made in 1D instead of 2D, but since this is linear optics it does not lose generality, this is, the conclusions will be the same.

3.1 Simulation tool

Originally, the system that was thought to represent in the simulator was simply a mirror, a receiver (sensor) and an emitter, but after some tests using this kind of system in the simulator, it was concluded that such a system would be impossible to implement in a real environment, so as a solution was placed a lens between the mirror and the sensor.

The simulator was designed in a way that some parameters are fixed and others could be changed, for different simulation scenarios. The fixed parameters are as follows,

- Mirror diameter,
- Field Stops of the Mirror, this serves to limit the FoV of the mirror.

The variable parameters are as follows,

- Tilt of the Mirror,
- Point Source position,
- Number of Point Sources,
- Distance between Point Sources,

- Lens Focal Length,
- Distance between Mirror and Lens,
- Sensor Size,
- Lens diameter.

Even though as will be demonstrated in chapter 3.2, the last three will be fixed parameters for the propose of this thesis.

3.1.1 System Design

As already mentioned, the first design of the system, was just a mirror, a receiver and a emitter, like it is represented of figure 3.3, but considering the FoV target of 0.0025°, this scheme was impossible to recreate on real environment, thus creating a problem, problem that will be described in section 3.2.

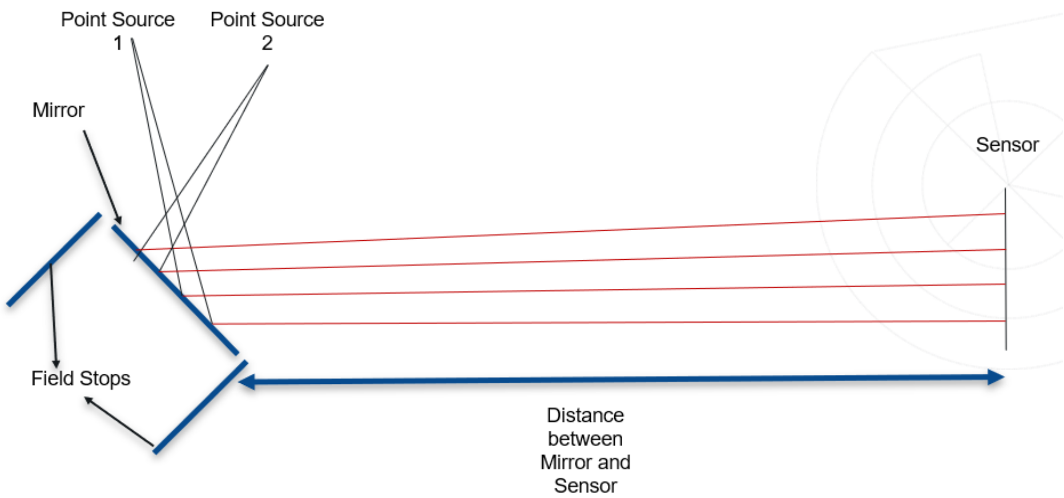

Figure 3.3: Initial simulation setup including a point source, mirror and a sensor.

So, with this problem in mind, a solution was found, a lens was added to the design, creating the final scheme in Figure 3.4.

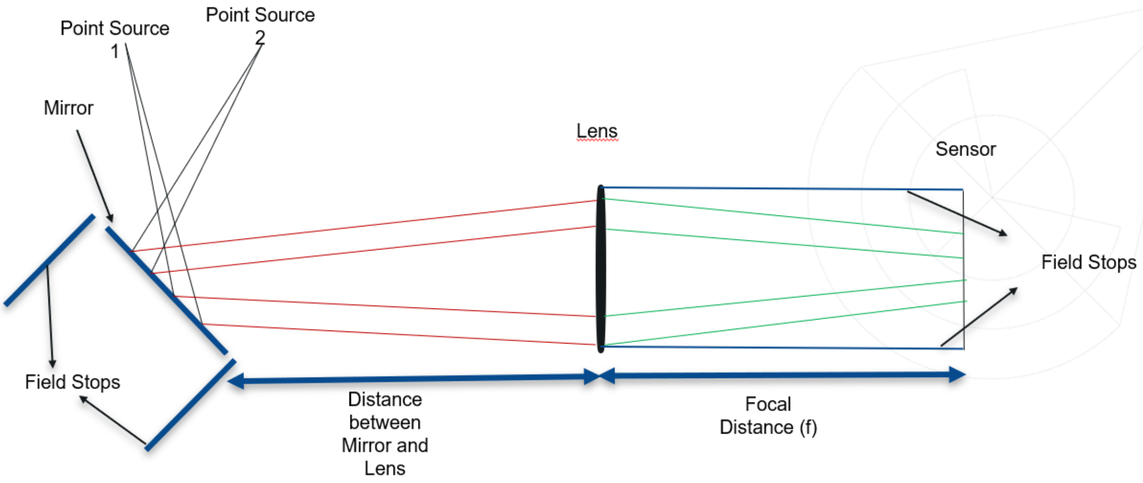

Figure 3.4: Second and final simulation setup including a Lens.

Before reaching the final simulation setup, the possibility of using a foldable setup was also considered, which consisted on using more than one mirror in order to get to the FoV of 0.0025°. Figure 3.5 is an example of a foldable setup. Since this setup required more than one mirror, and taking into account cost, this idea was abandoned.

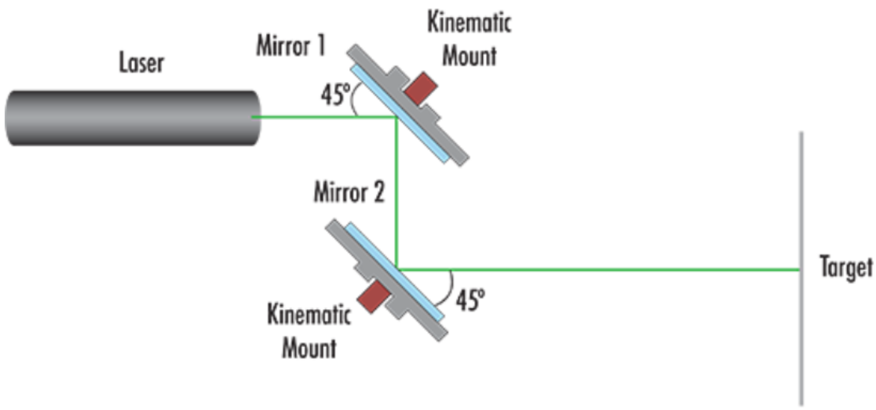

Figure 3.5: Foldable Setup example [38].

3.2 Using Simulation for defining parameters of the system

The first parameters that were defined were the ones that could not be changed, like the mirror diameter (15 mm) and the length of the Field Stops of the mirror. The later one is not specified in the datasheet of the mirror, however, a value of 9 mm is chosen since it fits in the mirror dimensions and it is less than the height of the mirror that is 15.52 mm . At the firs simulations, it was considered a sensor with a length of 5 cm, since it was not yet been chosen a commercial one. Later a sensor with a length of roughly 1.2 cm. The tilt of the mirror was also fixated at 45º for a better viewing.

Figure 3.3 depicts the initial simulation setup that does not include any lens. It was observed, using the simulator, that, in order to meet the required FoV, the distance between the mirror and the sensor should be around 140 meters, that is not viable for practical implementation. To avoid this technical impracticability, a lens was added between the mirror and the sensor.

After defining the design of second scheme, that is represented in Figure 3.4, it was necessary to find the ideal characteristics of the lens to be used. For some initial tests it was used an arbitrary diameter for the lens, 5 cm, while other lens were being studied. Then a lens was chosen, and this lens is discussed in the subsection 4.2.2. It was chosen a lens instead of an objective, because the later one would be more expensive, and it was possible to reach the objective of the thesis with only one lens.

Then, when all the values were finally defined, the value missing is the distance between the mirror and the lens. Tests were made to find the best value that would allow to reach the objective of the thesis. The simulation setup in the simulator made in Matlab is represented in Figure 3.6.

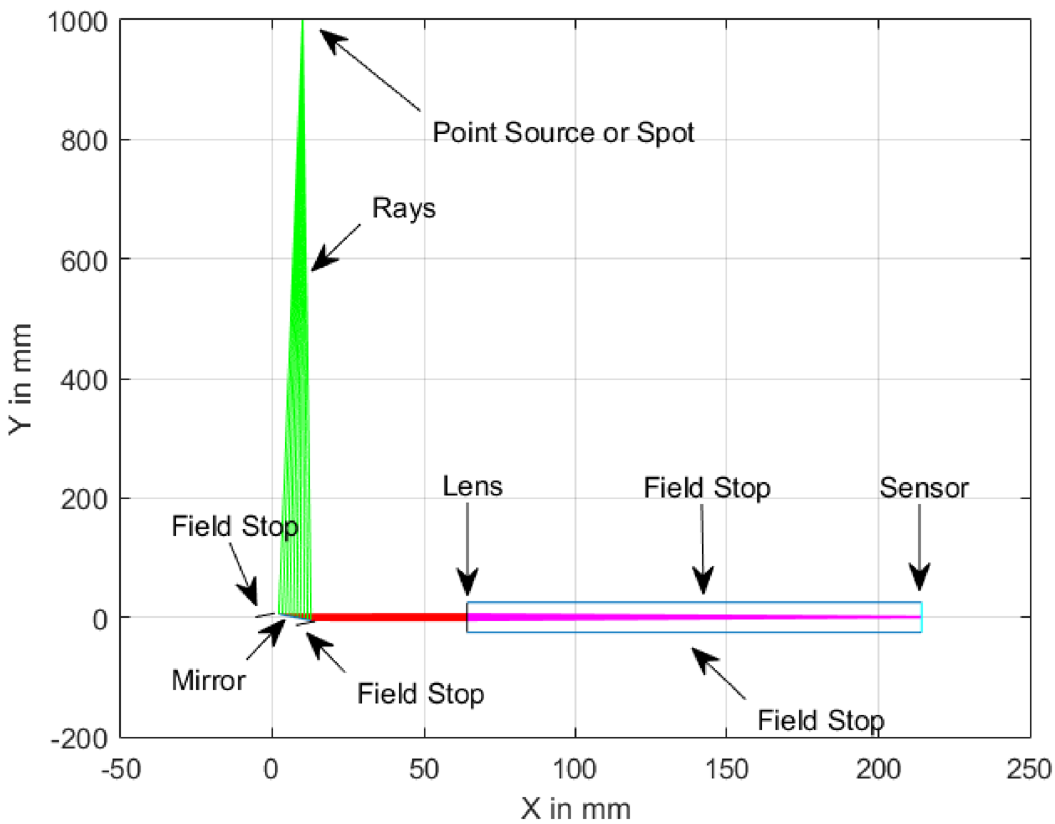

Figure 3.6: Simulation setup in Matlab.

CHAPTER 4

Numerical Performance

4.1 Initial tests

In these first tests to the simulator, the diameter of the lens and the sensor to be used were not yet defined, so the values to the diameter of the lens and the length of the sensor were defined as 5 cm. Also, at this time, the focal length of the lens was not also yet defined, so it was considered a value of 16 mm, based on [4]. These first tests objective, was mainly to test simulator.

4.1.1 Varying the distance between lens and mirror

In this test, the objective was to see what would be the gain (refracted rays that effectively reach the sensor) of the system varying the distance between mirror and lens. In Figure 4.1, it is possible to observe one of the cases simulated in order to obtain the gain of the system. For the preliminary simulations, it was considered that the sensor length and lens diameter have both 5 cm, since any of the hadn't yet been defined values at this point, as explained in chapter 3.

In the simulation, the distance between the spot and the mirror is 100 meters, and the spot had 10 mm wide. Figure 4.1 and 4.2 depicts two different scenarios where the point source starts at x=1 mm and x=10 mm respectively.

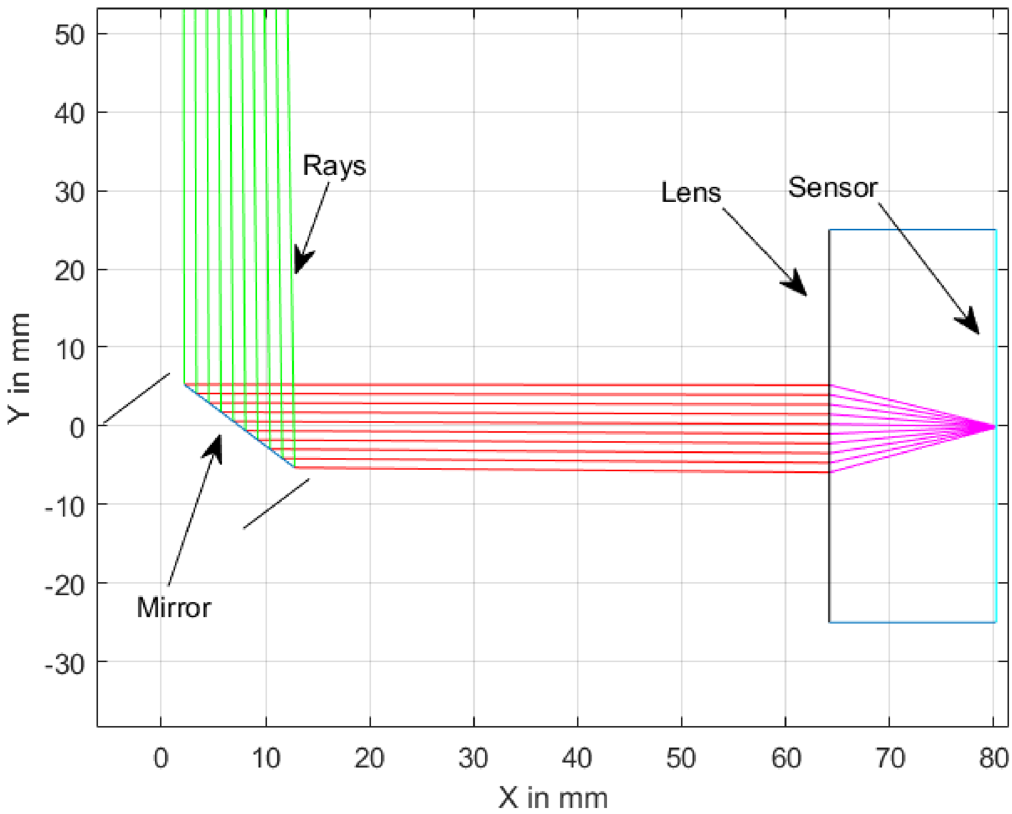

Figure 4.1: Enlarged Result of Simulation considering a spot distance 100m from the mirror and starting at x=1 mm and y=100 m.

As it is possible to observe in Table 4.1, regardless of the distance between the mirror and lens, all the rays emitted reach the sensor, so the gain in this case would always be 100%.

Distance between Mirror and Lens (cm)	Number of rays per spot	Hit	Miss	Gain(%)
5	10	100	0	100
15	10	100	0	100
25	10	100	0	100
35	10	100	0	100
50	10	100	0	100

Table 4.1: Gain as function of distance between mirror and lens, where point source starts at x=1 mm and y=100 m.

In the case represented in Table 4.2, as the distance between the mirror and lens increases, the number of rays reaching the sensor decreases, reaching 0 when that distance is 25 cm, and until 50 cm is still 0, which at this point starts to give an idea for the ideal distance between the Mirror and Lens, and also confirms that the FoV will influence the number of rays that reach the sensor.

Distance between Mirror and Lens (cm)	Number of rays per spot	Hit	Miss	Gain(%)
5	10	100	0	100
15	10	30	70	30
25	10	0	100	0
35	10	0	100	0
50	10	0	100	0

Table 4.2: Gain as function of distance between mirror and lens, where point source starts at x=100 mm and y=100 m.

4.1.2 Varying the length of the sensor

For the selection of sensor to be used, it was simulated the FoV as a function of the sensor length. In the simulation, it was considering that the distance between Mirror and Lens is 5 cm, considering the previous tests, and the Focal Length is 16 mm. In Figure 4.2, where in (a) the length of the sensor is 1mm and in (b) is 10mm, is possible to observe how it would look on the simulator.

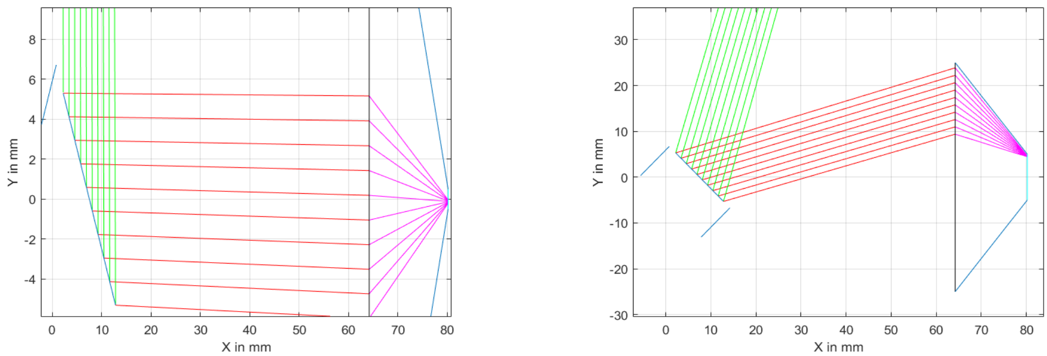

(a) Sensor with 1 mm length.

(b) Sensor with 10 mm length.

Figure 4.2: Simulation example to different sensor lengths.

Figure 4.3, shows the FoV variation with the length of the sensor, as this length increases, the value of the FoV also increases, until the length of the sensor is of 20 mm, where the value of the FoV, remains constant for lengths greater than 20 mm. Therefore, the smaller is the length of the sensor, the closer the objective is to be reached, also the conclusion can also be taken that from a certain length of the sensor this value won't influence the value of the FoV.

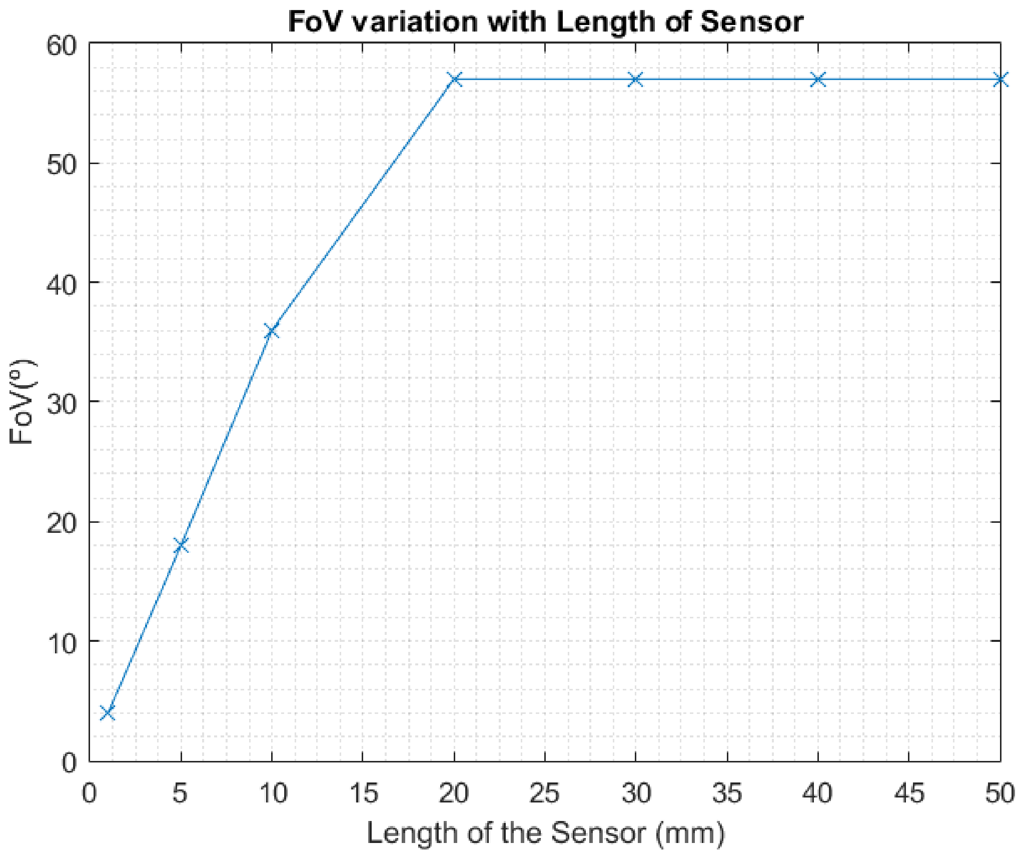

Figure 4.3: FoV variation with length of the sensor.

4.2 Tests to Find the Parameters Values

In these tests, the final parameters of the system were defined, namely: the distance between Mirror and Lens, the focal length and the length of the sensor.

Taking into account the tests made in the previous sub-chapter, where it was simulated the FoV as a function of the sensor, and considering the results of this simulation, where the FoV had a lower value when the sensor length is lower, it was chosen , as it was already mentioned in chapter 3, a sensor with a length of 1.2 cm, considering that one pixel as 5.86μm, so dividing the length of the sensor by the size of one pixel it's obtained the length of the sensor that roughly 2000 pixels. With this sensor it's easier to reach the required FoV, since it's possible to have the target FoV, considering the FoV per pixel, with this in mind the FoV is calculated as follows

$$FoVperPixel \approx \frac{FoVTotal}{numberofpixels} \tag{4.1}$$

Now the final value of the sensor length is chosen.

4.2.1 Distance Between Mirror and Lens

Considering the chosen sensor, now some tests to observe what would be the best value for the distance between the Mirror and Lens were made, considering the value of the focal length to be of 16 mm and the diameter of the lens of 5 cm, this values are still arbitrary, because at this point the lens was not yet chosen at this stage.

Figure 4.4 depicts the graphic of the FoV per pixels as a function of the distance between Mirror and Lens.

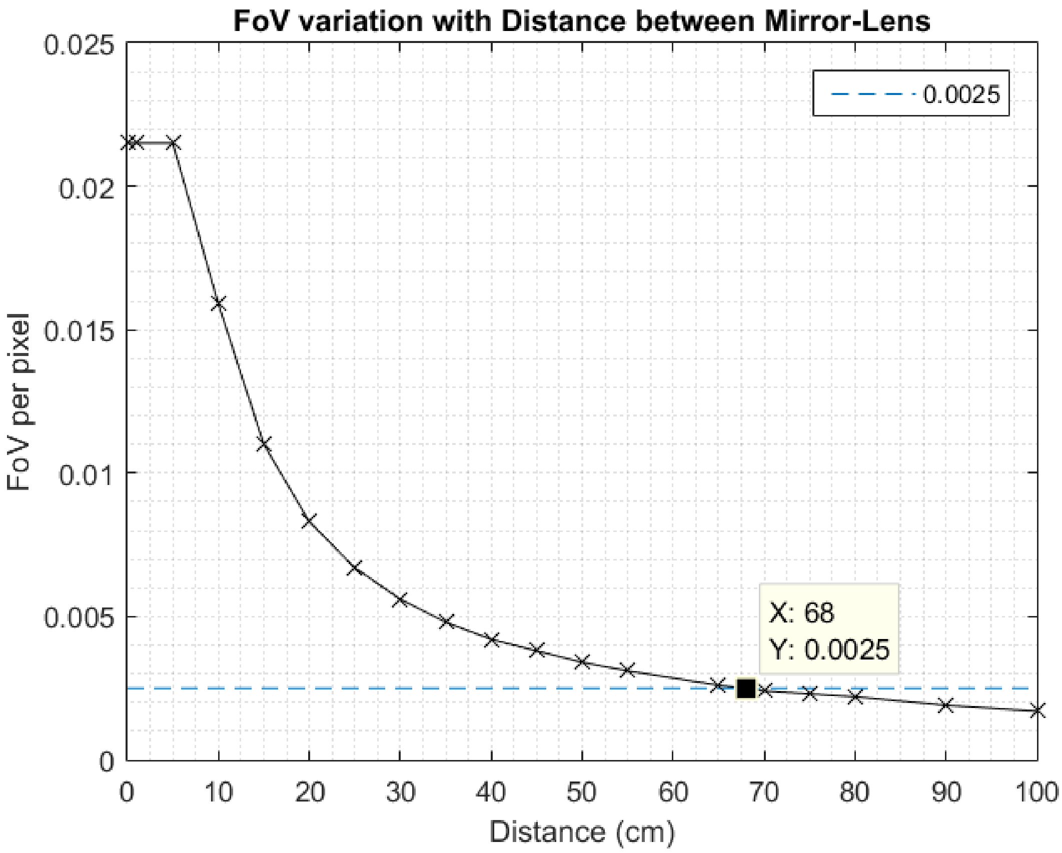

Figure 4.4: FoV variation with the distance between Mirror and Lens.

Observing Figure 4.4, the FoV per pixel from 0 to 5 cm is constant, this behaviour is due to the large size of the lens diameter. After 5 cm the FoV per pixel begins to decrease as the distance between the Mirror and Lens increases, resembling an exponential function. At this point, considering the values of the system, this means that the smaller the distance between the Mirror and the Lens, the better are the chances to reach the desired FoV per pixel. The FoV per pixel desired is obtained when the distance between the Mirror and Lens is 68 cm, which, considering this to be the distance used in the system, would give a total length of approximately 70 cm to the system, which is a considerable length for practical implementation. The smaller this value is, the better, so in that way the real setup of the system occupies less space.

4.2.2 Focal Length

Considering a fixed distance between the Mirror and Lens of 5 cm, a fixed diameter of the lens of 5 cm, the objective of this test was to observe how the FoV would change with the focal length. This variation is represented in Figure 4.5 where the values used for the focal length were values from various families of lens, since the lens was not yet chosen at this point this values were used just to see how the FoV would change with different values of focal length.

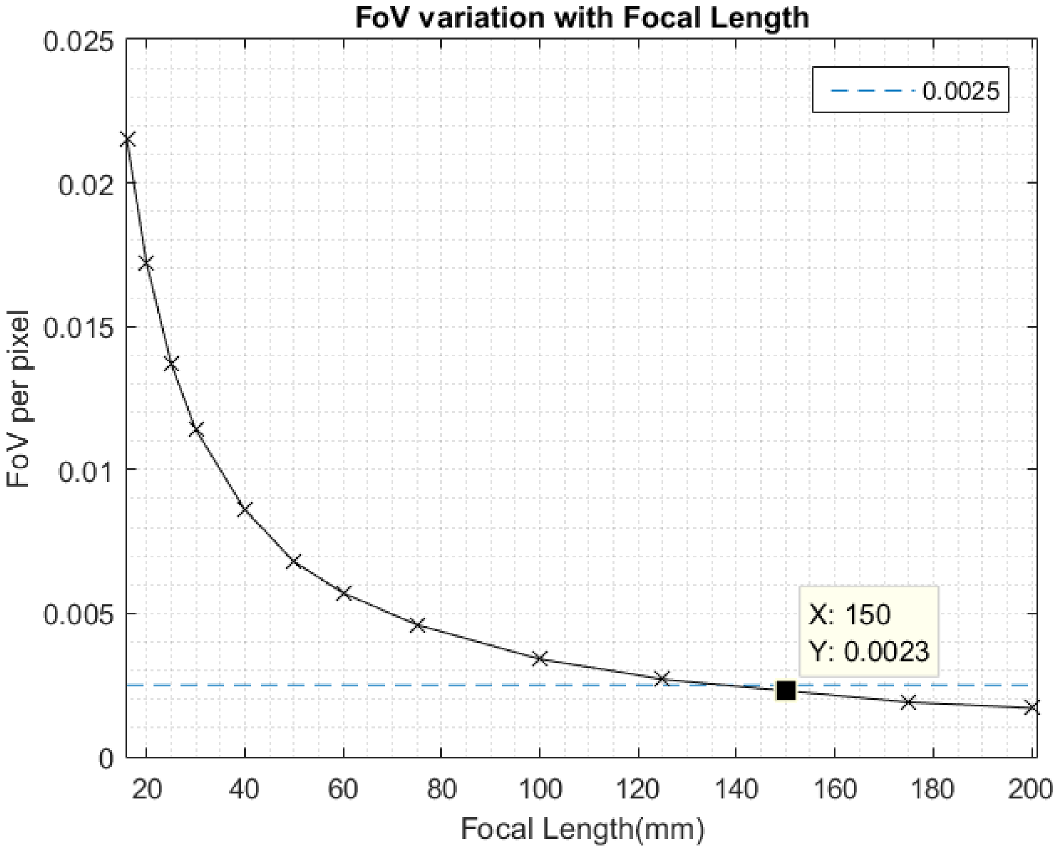

Figure 4.5: FoV variation with the Focal Length.

In Figure 4.5 is possible to observe that as the focal length increases, the value of FoV decreases, reaching the FoV per pixel of 0.0023° at a value of 150 mm for the focal length. Considering the values used for the focal length a FoV per pixel of 0.0023° since it is the closest FoV to the initial FoV target (0.0025°). So with this in mind, the FoV target now will be 0.0023°, since is the closest to the one first defined.

4.2.3 Tests to define the diameter of the lens

After searching available families of lens, it was selected a lens from the family of the N-BK7 Bi-Convex Lenses (AR Coating: 350 - 700 nm) [39], since this model is coated which reduces the reflection on the lens, and also has the possibility to chose between different focal lengths and different diameters for the lens. Since the value of this length isn't yet defined it is important to have different values to simulate.

The diameter chosen for testing was 1/2 inch (1.27 cm) and 1 inch (2.54 cm), that allows a far wide choice of focal lengths. The values used for the focal length are the ones represented in the description of the lens [39].

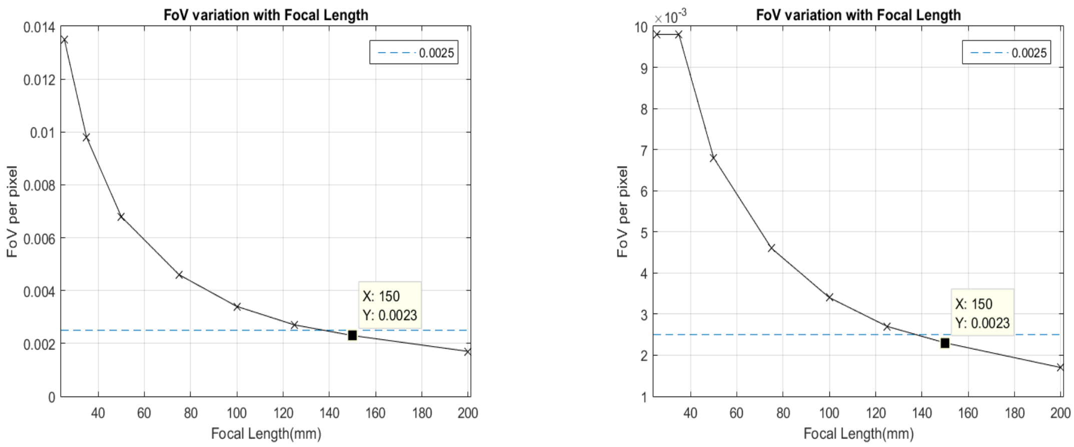

(a) Distance between Mirror and Lens of 5 cm. **(b)** Distance between Mirror and Lens of 10 cm.

Figure 4.6: FoV variation with Focal Length for a Lens with a diameter of 2.54 cm and a distance between Mirror and Lens of 5 cm and 10 cm.

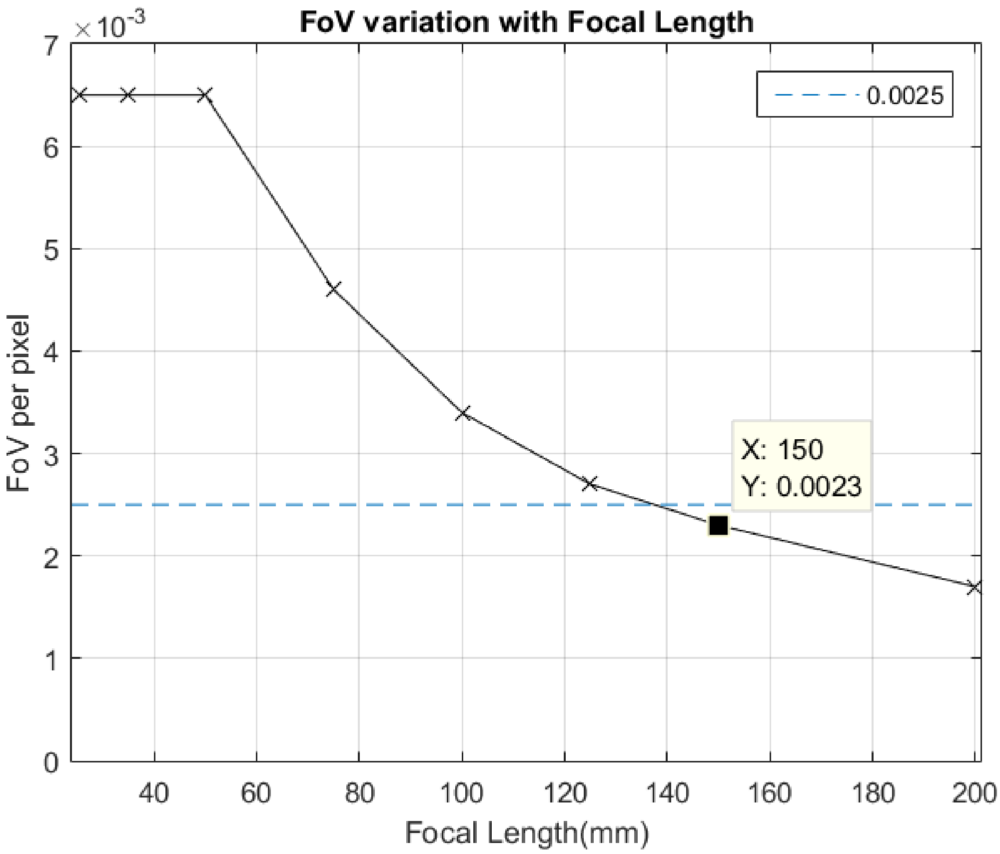

Figure 4.7: FoV variation with Focal Length for a Lens of diameter of 2.54 cm and a distance between Mirror and Lens of 15 cm.

In Figures 4.6, and 4.7, it's represented the graphics of the FoV variation with the focal length for a lens of 2.54 cm and three different values for the distance between Mirror and Lens, 5 cm, 10 cm and 15 cm. It is possible to observe that for the distances of 10 cm and 15 cm, the first values of the FoV per pixel is the same, this saturation happens because until the point when the FoV per pixel starts to decrease, the main factor that influences the value of the FoV is the distance between Mirror and Lens, and after that point, the value that starts to influence is the focal length. It is possible to see in Figure 4.6b that until and the second value considered for the focal length, the FoV is the same, and in Figure 4.7 this goes until the third value of focal length considered, which means the bigger is the distance between the Mirror and Lens the bigger will also be the value necessary for the focal length to influence the value of the FoV. When the focal length is the value influencing the FoV, the FoV tends to decrease as the focal length increases, and that happens in all the cases studied. The value 0.0023° for the FoV per pixel in all cases is reached when the focal length is 150 mm, and considering this it would be possible to have three setups, one with length of 20 cm when the distance between Mirror and Lens is 5 cm, other with 25 cm when the distance between Mirror and Lens is 10 cm and other of 30 cm when the distance between Mirror and Lens is 15 cm. Of the three, the best would be when the distance is 5 cm, once is the smaller length, that allows higher integration. And with that in mind, the next test, with a lens diameter of 1.27 cm was only made with a distance of 5 cm.

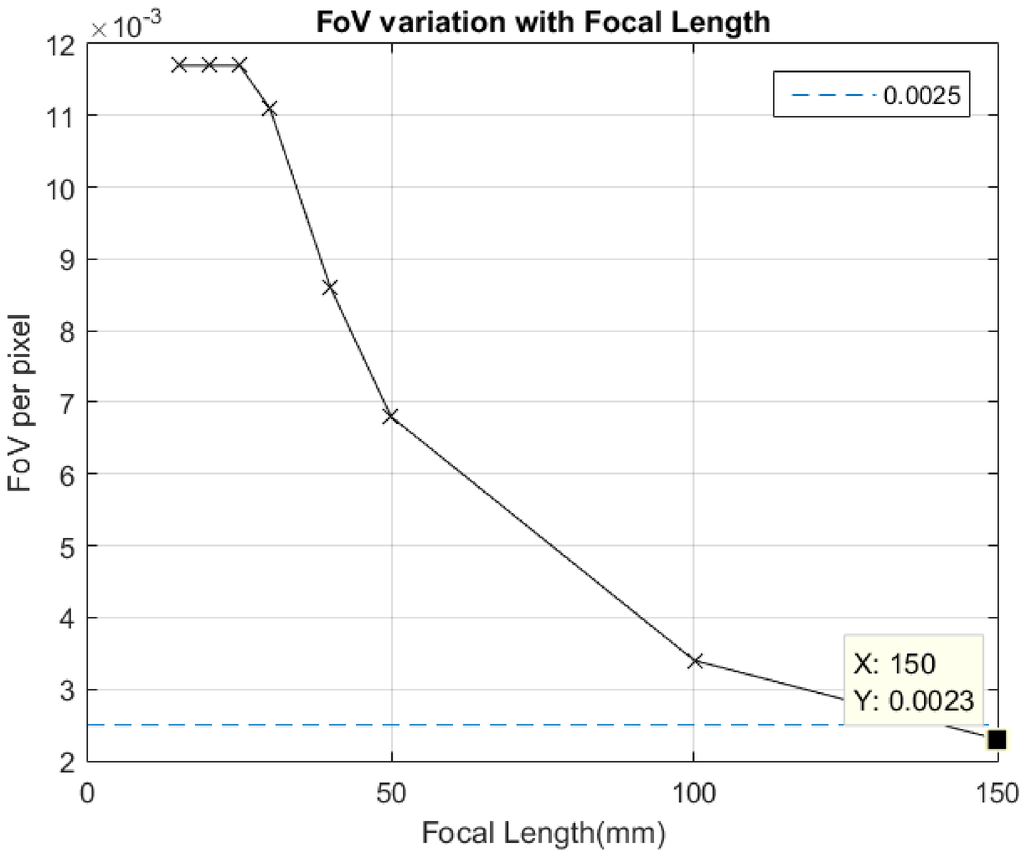

Figure 4.8: FoV variation for a Lens of diameter of 1.27 cm and a distance between Mirror and Lens of 5 cm.

The values used for the focal length were the ones in the description of the lens, [39], but for the diameter in question the focal would only go to 100 mm, but considering the simulation made represented in Figure4.8 a value for the focal length of 150 mm would also be necessary for the next simulations, and after consultation with the supervisors it was clarified that the focal length of 150 mm could also be chosen for that diameter.

Paying attention to Figure 4.8, the initial value of the FoV is the same for some values of the focal length, but in this case, the parameter that has more influence in the value of the FoV is the diameter of the lens. When the focal length is the value that influences the value of the FoV, the FoV per pixel decreases as the focal length increases, reaching the value of 0.0023° when the focal length is 150 mm.

The lens diameter chosen was 1.27 cm, once it occupies less space and it is cheaper than the diameter of 2.54 cm.

Since the best focal length of the Lens found in the previous tests is 150mm considering the diameter of the camera of 1.27 cm (1/2 inch), but, just for comparison with the values for the total length of the system, a new test with the value of the focal length being 15 mm, that is the lowest value possible for this lens, and varying the value of the distance between Mirror and Lens was made.

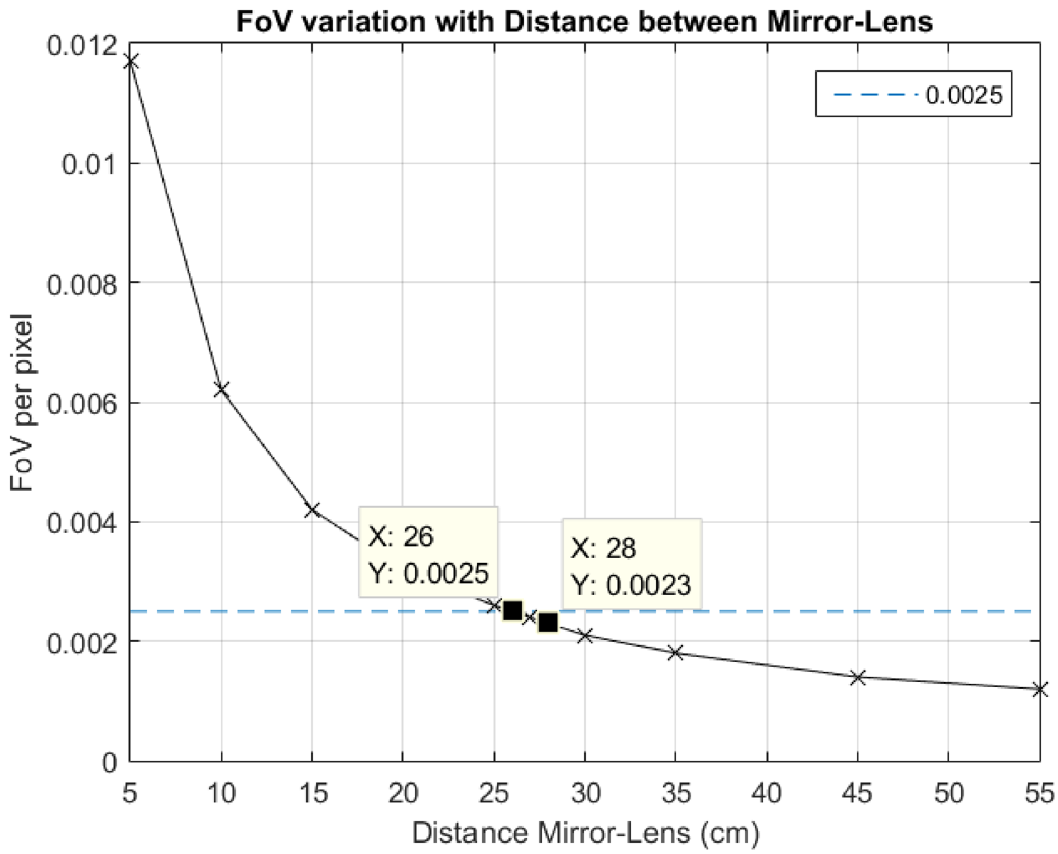

Figure 4.9: FoV variation with distance between Mirror and Lens.

As it is possible to observe in Figure 4.9, the FoV per pixel reaches the value of 0.0023º when the distance between the Mirror and Lens is 28cm, this gives a length to the system of

29.5 cm, also considering also the FoV per pixel of 0.0025°, this value is reached when the distance between Mirror and Lens is 26 cm, which gives a system with a length of 27.5 cm, and this two values are bigger than the distance of 20 cm already found in the tests with the focal length. So, a focal length value of 150 mm was considered the best solution.

4.2.4 Space Occupied on the Sensor

In order to verify if the spots were distinguishable on the sensor tests were made, where it was considered two pair of spots at a distance between them of 5 cm and a variable distance from the mirror, in order to watch how the size of the spots in the sensor would change. The two pairs considered represent two different situations, in one case the spot was just a point irradiating, this spot is considered to be a point source, since a point source is a "source of radiation concentrated at on point and has no spacial extension", and in the other case the spots had 1 cm thickness. It is important to remember that the sensor used has roughly 2000 pixels, and that one pixel has a length of 5.86μm.

First, it was considered the two point sources like it is represented on Figure 4.11a, and in Figure 4.10b is represented the close up on the sensor.

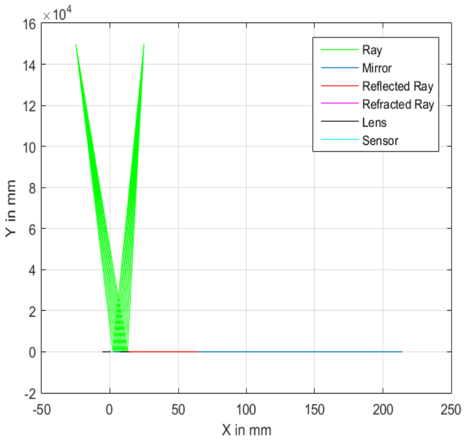

(a) Simulation with a pair of point sources.

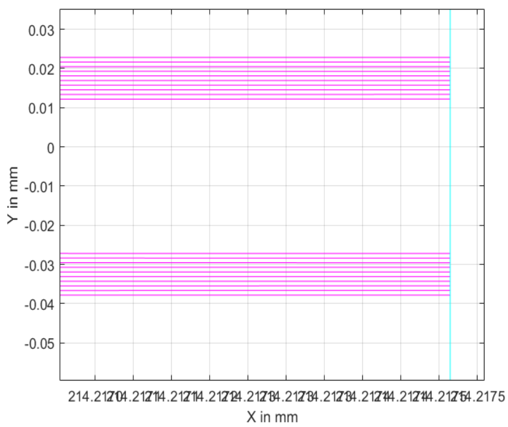

(b) Close up on the sensor.

Figure 4.10: Simulation with 2 point sources with a distance of 150m from the mirror.

Then, it was a considered the sources with thickness of 1cm. On Figure 4.11a it is possible to observe how the simulation looks for this case, and on Figure 4.11b is the close up on the sensor.

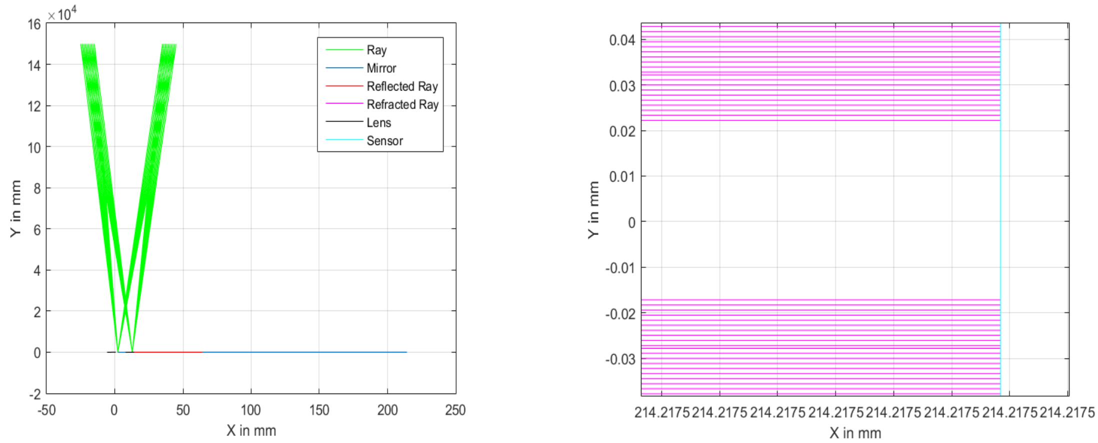

(a) Simulation with 2 spots with thickness of 1cm. **(b)** Close up on the sensor.

Figure 4.11: Simulation with 2 spots with 1cm thickness with a distance of 150m from the mirror.

In the first simulations were only used three values for the distance, 50m, 100m and 150m, the compilation of the space used in the sensor is represented in the the next tables.

Distance from the mirror (m)	Pair of Point Sources	Pair of Spots with 1 cm thickness
50	33 px	43 px
100	17 px	23 px
150	11 px	15 px

Table 4.3: Total Number of Pixels used by the two spots on the sensor.

Distance from the mirror (m)	Point Source	Spot with 1 cm thickness
50	6 px	11 px
100	3 px	6 px
150	2 px	4 px

Table 4.4: Total Number of Pixels used by an individual spot on the sensor.

Table 4.3 gives the total number of pixels used in the sensor. A pair of point sources from 50m occupies 33 pixels in total, the pair of spots of 1 cm thickness occupies 43 pixels, which means that a spot with 1 cm thickness occupies more space on the sensor than a point source. As the distance from the mirror increases, the space occupied on the sensor also decreases. The same happens in the pixels occupied by and individual spot, that it's shown on Table 4.4.

For the next tests, more distances were added, in order to see a better behavior of the relation between the distance from the mirror and the diameter that a spots occupies on the sensor. The distances added are between 25 m and 250 m.

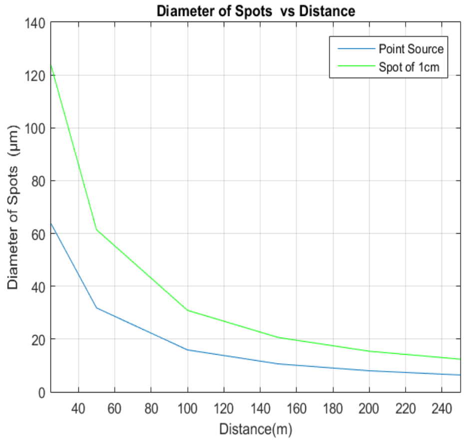

(a) Spot Diameter vs Distance.

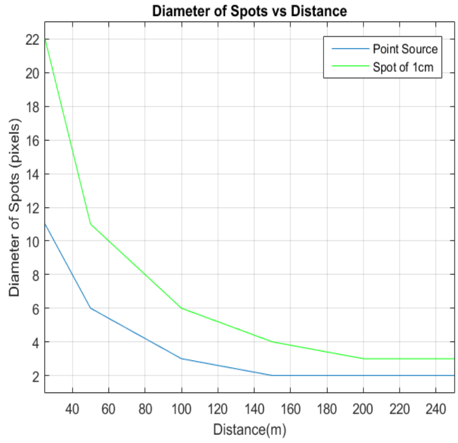

(b) Spot Diameter vs Distance.

Figure 4.12: Spot Diameter vs Distance in Pixels.

Figure 4.12a, depicts the graphic the variation of the diameter of the spot with the distance from the mirror, as it is possible to observe by analysing the graphic, as the distance from the mirror increases, the diameter of the spot in both cases simulated decrease. The diameter that a point source occupies on the sensor is smaller than the one that spot of 1 cm occupies, which makes sense, since the last is a bigger point source.

In Figure 4.12b, the relationship of the diameter with the distance is represented in a graphic and the units of the diameter that a spot occupies on the sensor is in pixels, and in order to obtain these values in pixels the values represented in Figure 4.12a were divided by the length of one pixel. At a distance of 25 m one spot of 1 cm occupies 22 pixels and one spot of a point source occupies 11 pixels, which, compared to the roughly 2000 pixels that the sensor has is not that much space occupied. As it was already seen on Figure 4.12, the curve in blue is referent to the point source, and the curve in green is referent to the spot with 1 cm of thickness. In the blue curve, when the distance from the mirror is 150m, the diameter of a point source occupies 2 pixels on the sensor, and from there to 250m the diameter used is always 2 pixels and the same happens in the green curve, this happens because it was used the command "ceil" on the values.

Now, in order to find the total space occupied by a pair of spots in both cases it is necessary to find out the spacing between the two spots on the sensor. This value are represented on Figure 4.13 and 4.13b in μm and in pixels, respectively.

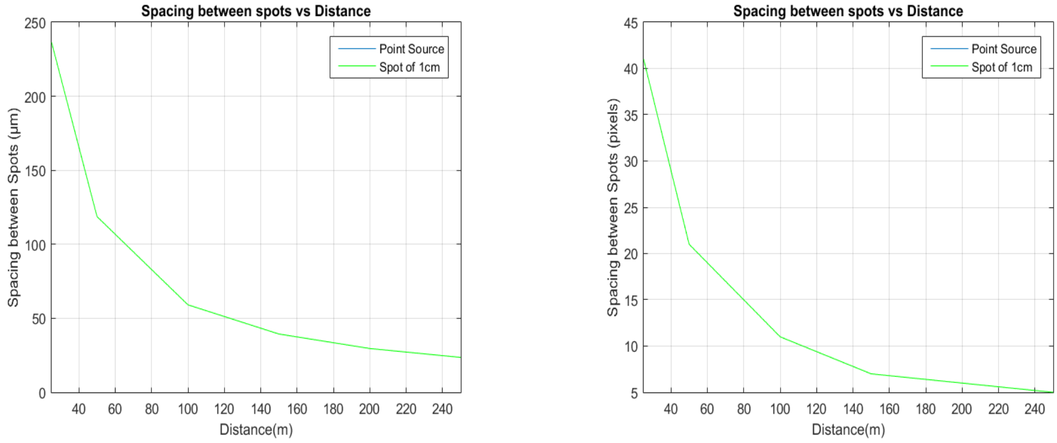

(a) Spacing between spots vs Distance. **(b)** Spacing between spots vs Distance in Pixels.

Figure 4.13: Spacing between spots vs Distance

Analysing the two figures it's possible to observe that the spacing in the both cases is the same. Which means that no matter the thickness of the point source, the spacing between them in the sensor will be the same. Therefore, both curves, Point Source and Spot, are overlaped, and it is only represented the curve in green. It's also possible to observe that as the distance from the mirror increases, the spacing between the spots in the sensor decreases.

In Figure 4.14, is represented all the space used by the 2 pair of spots sent with the variation of the distance from the mirror.

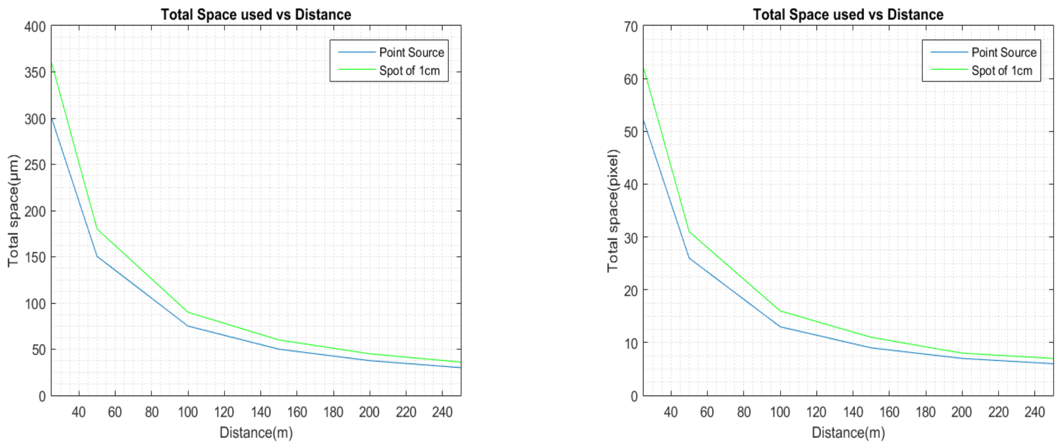

(a) Total Space Used vs Distance. **(b)** Total Space Used vs Distance in Pixels

Figure 4.14: Total Space Used vs Distance

As expected the space occupied by a pair of spots of thickness 1cm is bigger than the one occupied by the pair of point sources, even though the spacing between spots in the sensor was the same, the diameter of each spot was not, being that the diameter of the spot with 1 cm thickness occupies more space on the sensor, this can be seen on Figure 4.14a and on the Figure 4.14b.

These tests prove that it is possible to distinguish the spots on the sensor, and considering image resolution (detail that an image holds) in pixels, this tests show a great resolution, since for example, analyzing Figure 4.14b at 150 m a pair of point sources occupies roughly 10 pixels.

4.2.5 Focal length vs distance between mirror and lens vs FoV

By now all the parameters were supposedly defined, and for the last test, with a diameter of the lens defined, the focal length defined and also the sensor defined, it was made a test varying the distance between the Mirror and Lens and the focal length, in order to see how the FoV would behave. These values are represented in the Table 4.5, where Dist is the Distance between the Mirror and Lens, and FL is the focal length.

DIST / FL	1 cm	5 cm	10 cm	15 cm	20 cm	25 cm	26 cm	27 cm	30 cm	35 cm	50 cm	100 cm	150 cm	200 cm	250 cm
10mm	0,0311°	0,0117°	0,0062°	0,0042°	0,0032°	0,0026°	0,0025°	0,0024°	0,0021°	0,0018°	0,0013°	0,00064°	0,00042°	0,0003°	0,00024°
15mm	0,0229°	0,0117°	0,0062°	0,0042°	0,0032°	0,0026°	0,0025°	0,0024°	0,0021°	0,0018°	0,0013°	0,00064°	0,00042°	0,0003°	0,00024°
20mm	0,0171°	0,0117°	0,0062°	0,0042°	0,0032°	0,0026°	0,0025°	0,0024°	0,0021°	0,0018°	0,0013°	0,00064°	0,00042°	0,0003°	0,00024°
25mm	0,0138°	0,0117°	0,0062°	0,0042°	0,0032°	0,0026°	0,0025°	0,0024°	0,0021°	0,0018°	0,0013°	0,00064°	0,00042°	0,0003°	0,00024°
30mm	0,0114°	0,0111°	0,0062°	0,0042°	0,0032°	0,0026°	0,0025°	0,0024°	0,0021°	0,0018°	0,0013°	0,00064°	0,00042°	0,0003°	0,00024°
40mm	0,0086°	0,0086°	0,0062°	0,0042°	0,0032°	0,0026°	0,0025°	0,0024°	0,0021°	0,0018°	0,0013°	0,00064°	0,00042°	0,0003°	0,00024°
45mm	0,0076°	0,0076°	0,0062°	0,0042°	0,0032°	0,0026°	0,0025°	0,0024°	0,0021°	0,0018°	0,0013°	0,00064°	0,00042°	0,0003°	0,00024°
50mm	0,0068°	0,0068°	0,0062°	0,0042°	0,0032°	0,0026°	0,0025°	0,0024°	0,0021°	0,0018°	0,0013°	0,00064°	0,00042°	0,0003°	0,00024°
100mm	0,0034°	0,0034°	0,0034°	0,0034°	0,0034°	0,0026°	0,0025°	0,0024°	0,0021°	0,0018°	0,0013°	0,00064°	0,00042°	0,0003°	0,00024°
150mm	0,0023°	0,0023°	0,0023°	0,0023°	0,0023°	0,0023°	0,0023°	0,0023°	0,0021°	0,0018°	0,0013°	0,00064°	0,00042°	0,0003°	0,00024°

Table 4.5: FoV vs Distance between Mirror and Lens and Focal Length.

As it is possible to observe, in green are represented all the values where it is possible to get the FoV per pixel target 0.0025° or 0.0023°. Until now the value considered for the distance between the Mirror and Lens was 5 cm, but in this final test, it was possible to observe that even with the distance of 1 cm it would be possible to get the FoV target desired. Analysing the table, it is possible to get the FoV of 0.0025°, but the system would have a total length of 27 cm minimum, and considering 0.0023° the length of the system would be 16 cm minimum, even when it was considered 5 cm the total length would be 20 cm, which continues to be smaller than the minimal for a FoV of 0.0025°. Here it was also confirmed that the best value to use for the focal length of the lens is 150 mm, as it was assumed when choosing the ideal lens. So the final distance between the Mirror and Lens is 1 cm, and now all suitable parameters of the system were obtained.

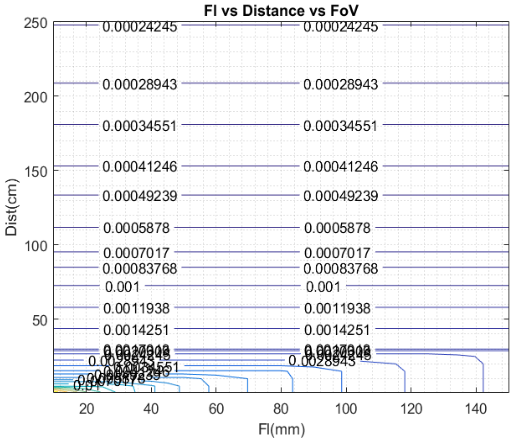

(a) Graphic of FoV vs Distance between Mirror and Lens and Focal Length.

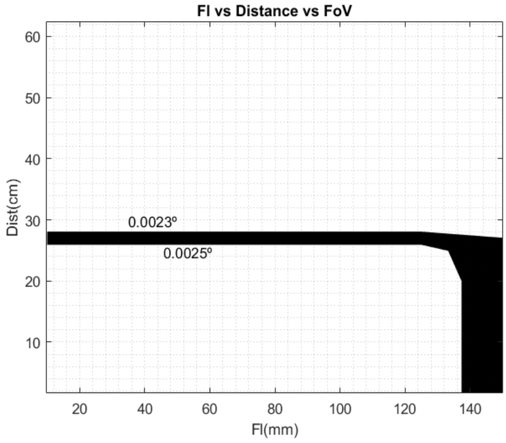

(b) Graphic of FoV vs Distance between Mirror and Lens and Focal Length.

Figure 4.15: Graphic of FoV vs Distance between Mirror and Lens and Focal Length.

In Figure 4.15 are represented two graphics considering the values on the table 4.5. In Figure 4.15b is the same graphic that is represented on Figure 4.15a, but only with the values for the FoV per pixel of 0.0023º and 0.0025 for a better viewing.

CHAPTER 5

Lidar Equation

Supposing a scenario during the day where there can be sunlight or even at night with the public lights and lights from other cars. These lights may influence the image on the sensor, working like a threshold to the intensity of light in each pixel, and this can make a spot or various spots less distinguishable, which can cause errors. For a better understanding of this problem and for find a solution to cases like this is important to study the Lidar Equation of the system. The maximum detectable distance of the system will depend on parameters like the transmitted power, the reflectively, atmospheric conditions, and all this can be combined in a Lidar Equation [4], given in 5.1, estimating the peak power of the signal that reaches the sensor.

$$P_r = P_t \times \frac{1}{4 \times \pi \times d^2} \times A_d \times \sigma, \tag{5.1}$$

Where P_r is the received power, P_t is the transmitted power, d is distance, A_d is the receiver aperture $[m^2]$ and σ is the reflectivity.

A single pixel corresponds to a determinate FoV, and assuming that the both horizontal and vertical FoV are equal, that the target is flat and at a distance "d"(m) from the receiver, that "I"($W.sr.m^2$) is the radiance of the background light and that "SW"(nm) is the spectral width to be considered, then the radius of a spot is given by the next equation,

$$r_{spot} = 2 \times d \times \tan \frac{FoV}{2}, \tag{5.2}$$

The corresponding spot area is then given by,

$$A_{spot} = \pi \times d^2 \times \tan \frac{FoV}{2}^2, \tag{5.3}$$

And the equation of the received power of the background light is given by,

$$P_{r,b} = A_s \times I \times SW \times \frac{1}{4 \times \pi \times d^2} \times A_r \times \sigma, \tag{5.4}$$

$$P_{r,b} = \frac{1}{4} \times \tan \frac{FoV}{2}^2 \times I \times SW \times A_r \times \sigma. \tag{5.5}$$

Also, in the equation of the received signal power, equation 5.1, this equation is also influenced by the spots area, which gives a new equation,

$$P_r = P_t \times \frac{1}{4 \times \pi \times d^2} \times A_d \times \frac{\sigma}{A_{spot}}. \tag{5.6}$$

For the simulation it was considered a spot with a transmitted power of 1 mW, the Receiver Aperture is calculated considering the diameter of the mirror, 15 mm, the Distance is from 0 to 300m and the FoV is 0.0023º. The equation used is 5.6, since it takes into account the influence of the spot area.

Figure 5.1 represents the behavior of the Lidar Equation with the Distance in a logarithmic scale. The signal received is represented in blue. The dashed curves represent the background light for the wavelengths 760, 905 and 1395 nm with colours black, green and red.

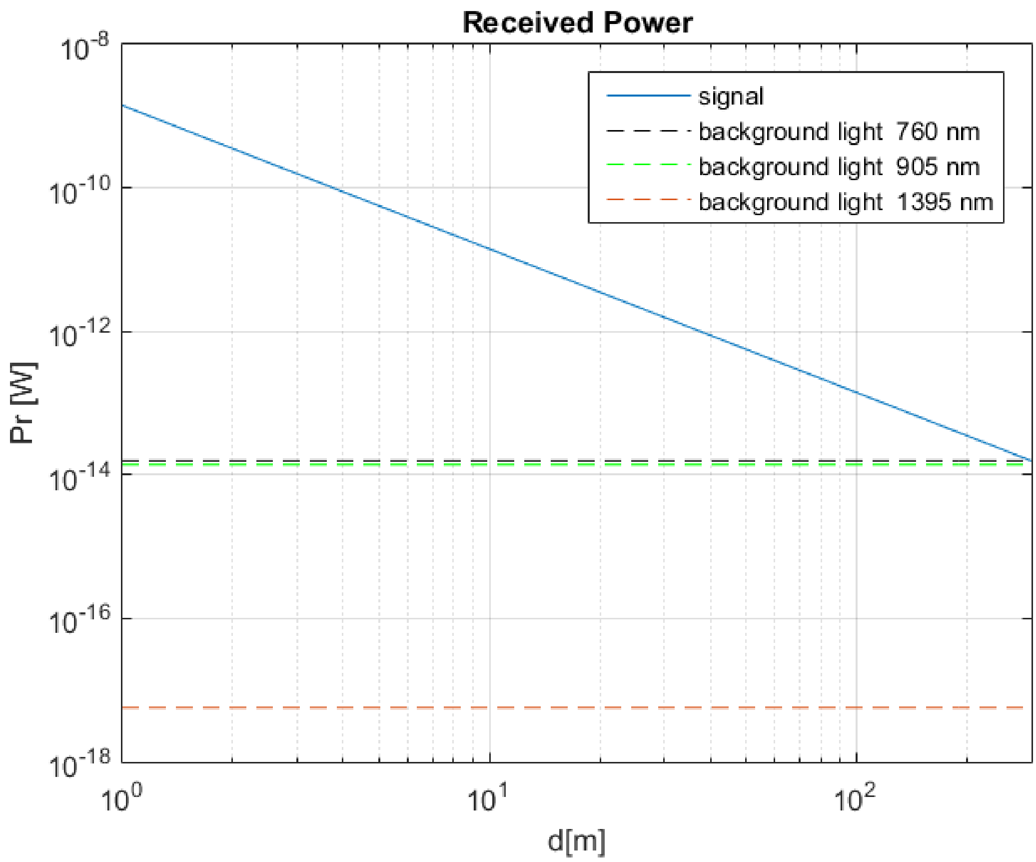

Figure 5.1: Received Power vs Distance.

As seen in the graphic, the signal will not have interference from the background light for all the wavelengths simulated, considering the distance of interest to this thesis. This means that the conceived system would work without the interference of background light, supporting then the use of a ROI LiDAR. The power received for the three wavelengths of background light considered is always constant because de received power is always the same.

CHAPTER 6

Conclusion

In order to simulate the concepts studied a simulation tool was developed and validated. The simulation tool was based on the developed system architecture. This system architecture consisted of one mirror, one lens and one sensor.

Throughout the development of the work, the simulation tool was validated and after that validation the parameters for the system were defined, considering the initial objective of proving that an ROI LiDAR works and finding a FoV of 0.0025°. For the setup, it was selected a dual-axis 2D mirror with position feedback from Optotune, the lens was from the family N-BK7 Bi-Convex Lenses (AR Coating: 350 - 700 nm), and some tests were conducted in order to find it's diameter considering all the focal lengths possible in each diameter, and the chosen sensor was a sensor with a length of roughly 2000 pixels.

While conducting test in order to find the parameters values of the system architecture, such as the distance between the Mirror and Lens and the focal length, it was found, that for an FoV with a value of 0.0025°, the system would have a total of 27 cm minimum. Still, considering that the FoV would be 0.0023°, the system would have a minimum length of 16 cm, which is much smaller than the value initially considered, so the FoV target was changed to 0.0023°. This value was reached when the distance between Mirror and Lens was 1 cm, and the focal length had a value of 150 mm, and this is perfectly doable and reasonable.

A LiDAR equation for the system was also developed in order to analyze the influence of background light in the system. With this equation, it was found that for a spot with a constant transmitted power, the system would have visibility considering the wavelengths simulated, which means that the systems would work without the interference of background light. This confirms that a ROI LiDAR would work in a real environment.

Even though it was not conducted a experimental validation of the simulation results, with the theoretical results obtained and conclusions from them, the main conclusion is that an ROI LiDAR is doable. Certainly, it is able to complement a triangulation based LiDAR. The ROI LiDAR can distinguish spots at great distances, the maximum error is lower that 1% as mentioned in the first chapter. The only problem with a ROI LiDAR would be the cost, since the mirror alone costs around 5000€, but with mass production of this kind of LiDAR the cost would certainly be reduced.

CHAPTER 7

Future Work

Having theoretically validated the proposed ROI LiDAR and the possibility of achieving a FoV of 0.0023°, the next step into validating the ROI LiDAR should be a experimental validation.

The experimental validation was initially planned to be done during the course of the thesis but, unfortunately, the mirror needed for the experimental validation did not arrive in time, it only arrived by the end of September, and so this thesis could not be supported by a experimental validation.

For the experimental validation it would be necessary the mirror with a programmable controller, the selected lens and sensor. For the realisation of tests, it would be only needed a laser to simulate a spot, and a computer for acquiring and processing the results.

Bibliography

[1] ASIRT, *Road safety facts*, Last accessed 11 July 2019, 2018. [Online]. Available: https://www.asirt.org/safe-travel/road-safety-facts/.

[2] *What is region of interest*, Last accessed 12 November 2019, [Online]. Available: https://www.igi-global.com/dictionary/avi-surface-flaws-manufactures/24858.

[3] K. A. Strand, *Parallax - optics*, Last accessed 11 July 2019, [Online]. Available: https://www.asirt.org/safe-travel/road-safety-facts/.

[4] R. Afonso, *Spatial domain lidar*, Mse Thesis, Universidade de Aveiro 2014, 2019.

[5] T. Dobbert, *Matchmoving: The Invisible Art of Camera Tracking*, 2nd ed. 2012, ISBN: 978-1-118-35205-2.

[6] D. M. Z. Zalevsky, *Optical super-resolution.* 2004, ISBN: 0-387-00591-9.

[7] J. Hendrickson, *What are the different self-driving car "levels" of autonomy?*, Last accessed 11 July 2019, 2019. [Online]. Available: https://www.howtogeek.com/401759/what-are-the-different-self-driving-car-levels-of-autonomy/.

[8] TERABEE, *Time of flight principle*, Last accessed 24 June 2019, [Online]. Available: https://www.terabee.com/time-of-flight-principle/.

[9] *What is a point cloud? what is lidar?*, Last accessed 24 June 2019, 2015. [Online]. Available: https://knowledge.safe.com/articles/257/what-is-a-point-cloud-what-is-lidar.html.

[10] G. Torbet, *Luminar's cheap lidar could be a big boost for autonomous vehicles*, Last accessed 24 June 2019, 2019. [Online]. Available: https://www.engadget.com/2019/07/12/luminar-affordable-lidar/?guccounter=1&guce_referrer=aHR0cHM6Ly93d3cuZ29vZ2xlLmNvbS8&guce_referrer_sig=AQAAAItPz_IwEXXaPvMk3KeuAum_R25sYRb-XCBCuh5FCFmTVfRU7Uh0tQkcua7gXw1IGjpinT_IKKm4PAczy0JbCNEkZdDrHLod3wmK6kD3tlyaViNctj5EwPuAjIW3rnTkKG8AwRF2zXddbAWODvQwmtQewdN_FW3UyWqDHqxx466n.

[11] Wikipedia, *Radar*, Last accessed 24 June 2019, [Online]. Available: https://en.wikipedia.org/wiki/Radar.

[12] M. Rouse, *Radar (radio detection and ranging)*, Last accessed 24 June 2019, 2005. [Online]. Available: https://searchmobilecomputing.techtarget.com/definition/radar.

[13] L. Critchley, *Lidar vs. radar*, Last accessed 24 June 2019, 2019. [Online]. Available: https://www.azooptics.com/Article.aspx?ArticleID=1527.

[14] *Cameras: The eyes of autonomous vehicles*, Last accessed 24 June 2019, 2017. [Online]. Available: https://sites.tufts.edu/jquinn/2017/10/10/cameras-the-eyes-of-autonomous-vehicles/.

[15] P. Pickering, *Radar and ultrasonic sensors strengthen adas object detection*, Last accessed 24 June 2019, 2017. [Online]. Available: https://www.electronicdesign.com/automotive/radar-and-ultrasonic-sensors-strengthen-adas-object-detection.

[16] Wikipedia, *Tesla autopilot*, Last accessed 17 June 2019, [Online]. Available: https://en.wikipedia.org/wiki/Tesla_Autopilot#History.

[17] V. Tabora, *Tesla enhanced autopilot overview — l2 self driving hw2*, Last accessed 17 June 2019, 2018. [Online]. Available: https://medium.com/self-driving-cars/tesla-enhanced-autopilot-overview-l2-self-driving-hw2-54f09fed11f1.

[18] Tesla, *Autopilot*, Last accessed 17 June 2019, [Online]. Available: https://www.tesla.com/autopilot?redirect=no.

[19] M. Liedtke and T. Krishner, *Tesla expects to have fully self-driving cars by next year*, Last accessed 17 June 2019, 2019. [Online]. Available: https://www.pbs.org/newshour/economy/tesla-set-to-unveil-fully-self-driving-car-technology.

[20] A. MediaCenter, *Automated driving at a new level: The audi ai traffic jam pilot*, Last accessed 24 June 2019, 2017. [Online]. Available: https://www.pbs.org/newshour/economy/tesla-set-to-unveil-fully-self-driving-car-technology.

[21] Waymo, *Technology*, Last accessed 18 June 2019, [Online]. Available: https://www.pbs.org/newshour/economy/tesla-set-to-unveil-fully-self-driving-car-technology.

[22] M. Fitzsimmons, *Waymo: Everything you need to know from google until now*, Last accessed 18 June 2019, 2018. [Online]. Available: https://www.techradar.com/news/waymo.

[23] S. Elnaj, *The uber accident, waymo technology and the future of self-driving cars*, Last accessed 18 June 2019, 2018. [Online]. Available: https://www.forbes.com/sites/forbestechcouncil/2018/05/24/the-uber-accident-waymo-technology-and-the-future-of-self-driving-cars/#2b1b81df7814.

[24] D. Robitzski, *Expert slams waymo safety data: "they obviously do not trust these numbers"*, Last accessed 18 June 2019, 2019. [Online]. Available: https://futurism.com/waymo-safety-data-trust-numbers.

[25] Wikipedia, *Uber*, Last accessed 18 June 2019, [Online]. Available: https://en.wikipedia.org/wiki/Uber.

[26] L. Johnson and M. Fitzsimmons, *Uber self-driving cars: Everything you need to know*, Last accessed 18 June 2019, 2018. [Online]. Available: https://www.techradar.com/news/uber-self-driving-cars.

[27] H. Xie, *MEMS Mirrors*. 2018, ISBN: 978-3-03842-868-8.

[28] *Mar1100 – mems 2d laser scanning mirror*, Last accessed 13 November 2019, [Online]. Available: http://www.maradin.co.il/products/mar1100-mems-2d-laser-scanning-mirror/.

[29] *Mems mirrors*, Last accessed 20 June 2019, [Online]. Available: https://www.mirrorcletech.com/wp/products/mems-mirrors/.

[30] *Mems mirrors*, Last accessed 13 November 2019, [Online]. Available: https://www.hamamatsu.com/eu/en/product/optical-components/mems-mirror/index.html.

[31] *Mar1100 – mems 2d laser scanning mirror*, Last accessed 13 November 2019, [Online]. Available: http://www.maradin.co.il/products/mar1100-mems-2d-laser-scanning-mirror/.

[32] *Mar1800*, Last accessed 13 November 2019, [Online]. Available: http://www.maradin.co.il/products/mar1800/.

[33] *Mems chip*, Last accessed 13 November 2019, [Online]. Available: http://www.en.zhisensor.com/?page_id=15622.

[34] *Dual axis mirror with position feedback*, MR-15-30, Optotune, 2012. [Online]. Available: https://www.optotune.com/products/beam-steering/2d-mirror-mr-15-30.

[35] W. J. Smith, *Modern Optical Engineering*, 3rd ed. McGraw-Hill, 2000, ISBN: 0-07-136360-2.

[36] D. H. Klus, *How We Came to Know the Cosmos: Light & Matter*. The Star Garden, February 7, 2018, 2018, ISBN: 978-1999877811.

[37] K. Gibbs, *Reflection (plane mirrors)*, Last accessed 25 July 2019, 2013. [Online]. Available: http://www.schoolphysics.co.uk/age16-19/Optics/Reflection/text/Reflection_/index.html.

[38] E. Optics, *Simplifying laser alignment*, Last accessed 14 February 2019, 2015. [Online]. Available: https://www.edmundoptics.com/resources/application-notes/lasers/simplifying-laser-alignment/.

[39] T. Labs, *N-bk7 bi-convex lenses (ar coating: 350 - 700 nm)*, Last accessed 14 February 2019. [Online]. Available: https://www.thorlabs.com/newgrouppage9.cfm?objectgroup_id=4848.

[40] *Point source*, Last accessed 11 July 2019, [Online]. Available: https://en.wikipedia.org/wiki/Point_source#Light.